SIAM J. NUMER. ANAL.
Vol. 48, No. 4, pp. 1281–1312

A MULTIPOINT FLUX MIXED FINITE ELEMENT METHOD ON HEXAHEDRA*

ROSS INGRAM†, MARY F. WHEELER‡, AND IVAN YOTOV†

Abstract. We develop a mixed finite element method for elliptic problems on hexahedral grids that reduces to cell-centered finite differences. The paper is an extension of our earlier paper for quadrilateral and simplicial grids [M. F. Wheeler and I. Yotov, *SIAM J. Numer. Anal.*, 44 (2006), pp. 2082–2106]. The construction is motivated by the multipoint flux approximation method, and it is based on an enhancement of the lowest order Brezzi–Douglas–Durán–Fortin (BDDF) mixed finite element spaces on hexahedra. In particular, there are four fluxes per face, one associated with each vertex. A special quadrature rule is employed that allows for local velocity elimination and leads to a symmetric and positive definite cell-centered system for the pressures. Theoretical and numerical results indicate first-order convergence for pressures and subface fluxes on sufficiently regular grids, as well as second-order convergence for pressures at the cell centers. Second-order convergence for face fluxes is also observed computationally.

Key words. mixed finite element, multipoint flux approximation, cell-centered finite difference, tensor coefficient, error estimates, hexahedra

AMS subject classifications. 65N06, 65N12, 65N15, 65N30, 76S05

DOI. 10.1137/090766176

1. Introduction.

In [48], the last two authors developed a special mixed finite element (MFE) method for elliptic problems, the multipoint flux mixed finite element (MFMFE) method, that reduces to cell-centered finite differences (CCFDs) on quadrilateral and simplicial grids and performs well for discontinuous full tensor coefficients. The goal of this paper is to develop and analyze a similar method for hexahedral grids.

MFE methods [15, 39] are widely used for the modeling of fluid flow and transport, as they provide accurate and locally mass conservative velocities and handle well discontinuous coefficients. In their standard form MFE methods require solving coupled pressure-velocity algebraic systems of saddle point type. To alleviate this problem, various modifications of the MFE method have been introduced. The hybrid MFE method [7, 15] can be reduced to a symmetric positive definite system for the pressure Lagrange multipliers on the element faces. In the case of the lowest order Raviart–Thomas (RT_0) MFE method [44, 38, 37], more efficient cell-centered formulations have also been developed; see [40, 46] for diagonal tensor coefficients and rectangular grids, as well as the expanded mixed finite element (EMFE) method for full tensor coefficients and general grids [5, 4]. The approach in these cell-centered methods is to diagonalize the mass matrix via appropriate quadrature rules, allowing for elimination of the velocities (see also [8] for a related method for triangular grids and diagonal tensor coefficients). Unfortunately the EMFE method suffers from de-

*Received by the editors July 27, 2009; accepted for publication (in revised form) June 9, 2010; published electronically August 19, 2010.

http://www.siam.org/journals/sinum/48-4/76617.html

†Department of Mathematics, University of Pittsburgh, Pittsburgh, PA 15260 (rni1@pitt.edu, yotov@math.pitt.edu). The first and the third authors were partially supported by the NSF grants DMS 0620402 and DMS 0813901 and the DOE grant DE-FG02-04ER25618.

‡Institute for Computational Engineering and Sciences, The University of Texas at Austin, Austin, TX 78712 (mfw@ices.utexas.edu). The second author was partially supported by the NSF grant DMS 0618679 and the DOE grant DE-FG02-04ER25617.

terioration of accuracy on discontinuous coefficients and rough grids, unless pressure Lagrange multipliers are introduced along discontinuous interfaces [4]. The computational cost of the EMFE method is comparable to the finite volume methods [23]. The latter also require certain orthogonality properties of the grid in the case of full tensor coefficients or need to be augmented with face-centered pressure Lagrange multipliers [24] to maintain optimal convergence. Further relationships between MFE and finite volume methods are established in [49].

Two other methods that are closely related to the RT_0 MFE method and perform well for rough grids and coefficients are the control volume MFE (CVMFE) method [18] and the mimetic finite difference (MFD) methods [28]. The relationship between these methods and the MFE method has been explored to analyze their convergence properties [29, 19, 41, 9, 11, 10, 17]. However, as in the case of MFE methods, both methods require solving algebraic saddle point problems in their standard form. Furthermore, MFE methods on polyhedral elements have been developed in [32, 33]; see also [42] for the analysis on hexahedra. The approach there is to subdivide the element into tetrahedra and use a piecewise affine approximation. Again, this formulation leads to an algebraic saddle point problem.

The multipoint flux approximation (MPFA) method [1, 2, 21, 22] has gained significant popularity in recent years since it combines the advantages of the abovementioned methods: it is accurate for rough grids and coefficients and reduces to a cell-centered stencil for the pressures. The method was originally developed as a nonvariational finite volume method. The analysis of the MPFA method has been done by formulating it as an MFE method with a special quadrature. In [48, 47], we developed the MFMFE method on quadrilateral and simplicial elements, which was motivated by and closely related to the MPFA method. Since the MPFA method uses subedge or subface fluxes to allow for local flux elimination, we considered the lowest order Brezzi–Douglas–Marini method, BDM_1 [14], which has similar velocity degrees of freedom. For example, the BDM_1 velocity space on quadrilaterals has a linear trace on each edge, thus two degrees of freedom per edge. We introduced a special quadrature rule for the velocity mass matrix, reducing it to a block-diagonal form, with blocks corresponding to the mesh vertices. As a result, the velocities could be eliminated, leading to a cell-centered system for the pressures. A closely related method on simplicial elements is proposed in [16]. An alternative approach on quadrilaterals is developed in [30] using a broken Raviart–Thomas (RT) space with a piecewise constant trace on each edge. The analyses in [48] and [30] on quadrilaterals are for the symmetric version of the MPFA method and require for optimal convergence that the elements are $O(h^2)$-perturbations of parallelograms. The numerical studies in [3] confirm these theoretical results. In [31], the nonsymmetric version of the MPFA method is studied, and convergence is shown for general quadrilaterals. A nonsymmetric MFD method on polyhedral elements that reduces to a cell-centered pressure system using an MPFA-type velocity elimination is developed and analyzed in [35].

In this paper we develop the MFMFE method on hexahedral elements. The method is designed to handle full tensor coefficients. The construction follows the approach in [48]. We consider the BDM_1 spaces on hexahedra. The BDM spaces were defined on bricks in [13], and we will refer to them as the BDDF spaces. Here we use their extension to hexahedra via the Piola transformation. We further enhance the BDDF_1 space in the following way. The original BDDF_1 velocity space on bricks has a linear normal velocity trace on each element face, thus three degrees of freedom per face. The MPFA construction requires four subface fluxes, one associated with each vertex of the face. We enhance the BDDF_1 velocity space by adding six curl

basis functions. The resulting space has bilinear normal traces on the faces, thus four degrees of freedom per face. We then formulate an MFE method using the enhanced BDDF_1 spaces on hexahedra and a special trapezoidal-based quadrature rule that allows for a local elimination of the velocities. The quadrature rule couples only velocity degrees of freedom associated with the same mesh vertex, leading to a block-diagonal mass matrix with 12×12 blocks corresponding to the mesh vertices. Solving the local linear systems allows for eliminating the 12 velocities in terms of the cell-centered pressures in the eight elements that share the vertex. The resulting system for the pressure is symmetric and positive definite and has a 27 point stencil.

The well-posedness and error analysis of the method are based on combining MFE analysis tools with quadrature error analysis. The error analysis requires approximation properties for RT_0 and BDDF_1 spaces on hexahedra. While such properties on quadrilaterals are well understood (see, e.g., [44, 15, 45, 6]), there is very limited analysis available for hexahedra. It was observed in [36] that the RT_0 velocity space does not contain the space of constant vectors on general hexahedra. As a result certain restrictive assumptions on the elements are needed to establish satisfactory approximation properties. Here we prove first order approximation in the $H(\mathrm{div})$-norm for RT_0 and BDDF_1 on elements that are $O(h^2)$-perturbations of parallelepipeds. Under an additional regularity assumption, second-order approximation in the L^2-norm is shown for BDDF_1. These results are established via mapping to the reference element and require careful bounds for the Piola transformation on hexahedra. We then prove first-order convergence for the MFMFE pressure in the L^2-norm and the velocity in the $H(\mathrm{div})$-norm. We also employ a duality argument to establish second-order convergence for the pressure at the cell centers under the additional regularity assumption. The theoretical results are verified numerically. We show that the geometry restriction on the elements is not just an artifact of the analysis, as we observe deterioration in the convergence order when the element regularity is reduced. We also compare the MFMFE method to the EMFE method and show that the former outperforms the latter on discontinuous coefficients and rough grids, as predicted by the theory.

The rest of the paper is organized as follows. The method is developed in section 2. Error analysis of the velocity and the pressure is given in sections 3 and 4, respectively. Numerical experiments are presented in section 5.

2. Definition of the method.

2.1. Preliminaries. We consider the second-order elliptic problem written as a system of two first-order equations,

$$\mathbf{u} = -K\nabla p \quad \text{in } \Omega, \tag{2.1}$$

$$\nabla \cdot \mathbf{u} = f \quad \text{in } \Omega, \tag{2.2}$$

$$p = g \quad \text{on } \Gamma_D, \tag{2.3}$$

$$\mathbf{u} \cdot \mathbf{n} = 0 \quad \text{on } \Gamma_N, \tag{2.4}$$

where $\Omega \subset \mathbb{R}^3$ is a polyhedral domain with a Lipschitz continuous boundary $\partial\Omega = \overline{\Gamma}_D \cup \overline{\Gamma}_N$, $\Gamma_D \cap \Gamma_N = \emptyset$, measure$(\Gamma_D) > 0$, $\mathbf{n}$ is the outward unit normal on $\partial\Omega$, and K is a symmetric, uniformly positive definite tensor satisfying, for some $0 < k_0 \le k_1 < \infty$,

$$k_0 \xi^T \xi \le \xi^T K(\mathbf{x}) \xi \le k_1 \xi^T \xi \quad \forall \mathbf{x} \in \Omega \ \forall \xi \in \mathbb{R}^3. \tag{2.5}$$

In flow in porous media modeling, p is the pressure, $\mathbf{u}$ is the Darcy velocity, and K represents the permeability divided by the viscosity. The choice of boundary condi-

tions is made for the sake of simplicity. More general boundary conditions can also be treated. We assume that the source $f \in L^2(\Omega)$ and the boundary data $g \in H^{1/2}(\Gamma_D)$ (see the notation below).

Throughout this paper, C denotes a generic positive constant that is independent of the discretization parameter h. For a domain $G \subset \mathbb{R}^3$, the $L^2(G)$ inner product and norm for scalar and vector-valued functions are denoted $(\cdot,\cdot)_G$ and $\|\cdot\|_G$, respectively. The norms and seminorms of the Sobolev spaces $W^{k,p}(G)$, $k \in \mathbb{R}$, $p > 0$, are denoted by $\|\cdot\|_{k,p,G}$ and $|\cdot|_{k,p,G}$, respectively. The norms and seminorms of the Hilbert spaces $H^k(G)$ are denoted by $\|\cdot\|_{k,G}$ and $|\cdot|_{k,G}$, respectively. We omit G in the subscript if $G = \Omega$. For a section of the domain or element boundary $S \subset \mathbb{R}^2$ we write $\langle\cdot,\cdot\rangle_S$ and $\|\cdot\|_S$ for the $L^2(S)$ inner product (or duality pairing) and norm, respectively. For a tensor-valued function M, let $\|M\|_\alpha = \max_{i,j} \|M_{ij}\|_\alpha$ for any norm $\|\cdot\|_\alpha$. The natural space for the velocity is

$$H(\mathrm{div};\Omega) = \{\mathbf{v} \in (L^2(\Omega))^3 : \nabla\cdot\mathbf{v} \in L^2(\Omega)\}$$

equipped with the norm

$$\|\mathbf{v}\|_{\mathrm{div}} = (\|\mathbf{v}\|^2 + \|\nabla\cdot\mathbf{v}\|^2)^{1/2}.$$

Let

$$\mathbf{V} = \{\mathbf{v} \in H(\mathrm{div};\Omega) : \mathbf{v}\cdot\mathbf{n} = 0 \text{ on } \Gamma_N\}, \quad W = L^2(\Omega).$$

The weak formulation of (2.1)–(2.4) is as follows: find $\mathbf{u} \in \mathbf{V}$ and $p \in W$ such that

$$(K^{-1}\mathbf{u},\mathbf{v}) = (p,\nabla\cdot\mathbf{v}) - \langle g,\mathbf{v}\cdot\mathbf{n}\rangle_{\Gamma_D}, \quad \mathbf{v} \in \mathbf{V}, \tag{2.6}$$

$$(\nabla\cdot\mathbf{u},w) = (f,w), \quad w \in W. \tag{2.7}$$

It is well known [15, 39] that (2.6)–(2.7) has a unique solution.

2.2. A finite element mapping. Let $\mathcal{T}_h$ be a finite element partition of Ω consisting of hexahedra, where $h = \max_{E\in\mathcal{T}_h} \mathrm{diam}(E)$. We assume that $\mathcal{T}_h$ is shape regular and quasi-uniform [20]. For any element $E \in \mathcal{T}_h$ there exists a trilinear bijection mapping $F_E : \hat{E} \to E$, where $\hat{E}$ is the reference cube. Denote the Jacobian matrix by DF_E, and let $J_E = |\det(DF_E)|$. Denote the inverse mapping by F_E^{-1}, its Jacobian matrix by DF_E^{-1}, and let $J_{F_E^{-1}} = |\det(DF_E^{-1})|$. We have that

$$DF_E^{-1}(\mathbf{x}) = (DF_E)^{-1}(\hat{\mathbf{x}}), \qquad J_{F_E^{-1}}(\mathbf{x}) = \frac{1}{J_E(\hat{\mathbf{x}})}.$$

The reference element $\hat{E}$ is the unit cube with vertices $\hat{\mathbf{r}}_1 = (0,0,0)^T$, $\hat{\mathbf{r}}_2 = (1,0,0)^T$, $\hat{\mathbf{r}}_3 = (1,1,0)^T$, $\hat{\mathbf{r}}_4 = (0,1,0)^T$, $\hat{\mathbf{r}}_5 = (0,0,1)^T$, $\hat{\mathbf{r}}_6 = (1,0,1)^T$, $\hat{\mathbf{r}}_7 = (1,1,1)^T$, and $\hat{\mathbf{r}}_8 = (0,1,1)^T$. Denote by $\mathbf{r}_i = (x_i, y_i, z_i)^T$, $i = 1,\dots,8$, the corresponding vertices of element E as shown in Figure 1. The outward unit normal vectors to the faces of E and $\hat{E}$ are denoted by $\mathbf{n}_i$ and $\hat{\mathbf{n}}_i$, $i = 1,\dots,6$, respectively. We will also use the notation $\mathbf{n}_e$ and $\hat{\mathbf{n}}_{\hat{e}}$ for the outward unit normals on faces e and $\hat{e}$, respectively. The trilinear mapping F_E is given, for $\hat{\mathbf{x}} = (\hat{x},\hat{y},\hat{z}) \in \hat{E}$, by

$$\begin{aligned} F_E(\hat{\mathbf{x}}) &= \mathbf{r}_1(1-\hat{x})(1-\hat{y})(1-\hat{z}) + \mathbf{r}_2\hat{x}(1-\hat{y})(1-\hat{z}) + \mathbf{r}_3\hat{x}\hat{y}(1-\hat{z}) + \mathbf{r}_4(1-\hat{x})\hat{y}(1-\hat{z}) \\ &\quad + \mathbf{r}_5(1-\hat{x})(1-\hat{y})\hat{z} + \mathbf{r}_6\hat{x}(1-\hat{y})\hat{z} + \mathbf{r}_7\hat{x}\hat{y}\hat{z} + \mathbf{r}_8(1-\hat{x})\hat{y}\hat{z} \\ &= \mathbf{r}_1 + \mathbf{r}_{21}\hat{x} + \mathbf{r}_{41}\hat{y} + \mathbf{r}_{51}\hat{z} + (\mathbf{r}_{34}-\mathbf{r}_{21})\hat{x}\hat{y} + (\mathbf{r}_{65}-\mathbf{r}_{21})\hat{x}\hat{z} + (\mathbf{r}_{85}-\mathbf{r}_{41})\hat{y}\hat{z} \\ &\quad + ((\mathbf{r}_{21}-\mathbf{r}_{34}) - (\mathbf{r}_{65}-\mathbf{r}_{78}))\hat{x}\hat{y}\hat{z}, \end{aligned} \tag{2.8}$$

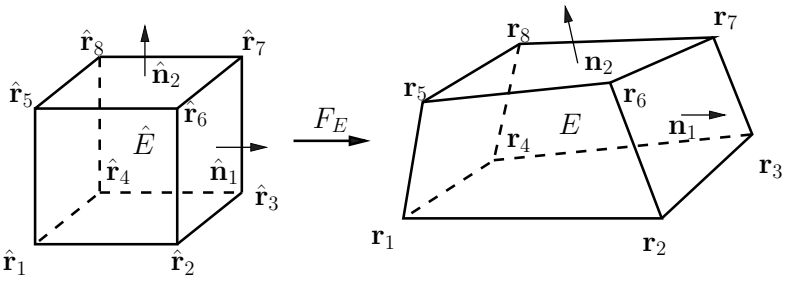

FIG. 1. *Trilinear hexahedral mapping.*

where $\mathbf{r}_{ij} = \mathbf{r}_i - \mathbf{r}_j$. We note that the elements can have nonplanar faces. Let $\hat{\phi}(\hat{\mathbf{x}})$ be defined on $\hat{E}$, and let $\phi = \hat{\phi} \circ F_E^{-1}$. Using the classical formula $\nabla\phi = (DF_E^{-1})^T\hat{\nabla}\hat{\phi}$, it is easy to see that for any face $e_i \subset \partial E$

$$\mathbf{n}_i = \frac{1}{|J_{e_i}|} J_E (DF_E^{-1})^T \hat{\mathbf{n}}_i, \quad J_{e_i} = |J_E (DF_E^{-1})^T \hat{\mathbf{n}}_i|_{\mathbb{R}^3}. \tag{2.9}$$

It is also easy to see that the mapping definition (2.8) and the shape-regularity and quasi-uniformity of the grids imply that

$$\begin{aligned} &\|DF_E\|_{0,\infty,\hat{E}} \le Ch, \quad \|J_E\|_{0,\infty,\hat{E}} \le Ch^3, \quad \|DF_E^{-1}\|_{0,\infty,E} \le Ch^{-1}, \\ &\qquad\qquad \text{and} \quad \|J_{F_E^{-1}}\|_{0,\infty,E} \le Ch^{-3} \quad \forall\, E \in \mathcal{T}_h. \end{aligned} \tag{2.10}$$

2.3. MFE spaces. Let $\mathbf{V}_h \times W_h$ be the lowest order BDDF_1 MFE spaces on hexahedra [14, 13, 15]. On the reference unit cube these spaces are defined as

(2.11)

$$\begin{aligned} \hat{\mathbf{V}}(\hat{E}) &= P_1(\hat{E})^3 + r_0\ \text{curl}(0,0,\hat{x}\hat{y}\hat{z})^T + r_1\ \text{curl}(0,0,\hat{x}\hat{y}^2)^T + s_0\ \text{curl}(\hat{x}\hat{y}\hat{z},0,0)^T \\ &\quad + s_1\ \text{curl}(\hat{y}\hat{z}^2,0,0)^T + t_0\ \text{curl}(0,\hat{x}\hat{y}\hat{z},0)^T + t_1\ \text{curl}(0,\hat{x}^2\hat{z},0)^T \\ &= P_1(\hat{E})^3 + r_0(\hat{x}\hat{z},-\hat{y}\hat{z},0)^T + r_1(2\hat{x}\hat{y},-\hat{y}^2,0)^T + s_0(0,\hat{x}\hat{y},-\hat{x}\hat{z})^T \\ &\quad + s_1(0,2\hat{y}\hat{z},-\hat{z}^2)^T + t_0(-\hat{x}\hat{y},0,\hat{y}\hat{z})^T + t_1(-\hat{x}^2,0,2\hat{x}\hat{z})^T, \\ \hat{W}(\hat{E}) &= P_0(\hat{E}), \end{aligned}$$

where r_i, s_i, and t_i, $i = 0, 1$, are real constants and P_k denotes the space of polynomials of degree $\le k$. Note that the curl terms above have been added so that

$$\hat{\nabla}\cdot\hat{\mathbf{V}}(\hat{E}) = \hat{W}(\hat{E}), \quad \text{and} \quad \forall\,\hat{\mathbf{v}} \in \hat{\mathbf{V}}(\hat{E}),\ \forall\,\hat{e} \subset \partial\hat{E},\ \hat{\mathbf{v}}\cdot\hat{\mathbf{n}}_{\hat{e}} \in P_1(\hat{e}).$$

There are other possibilities for augmenting $P_1(\hat{E})^3$ to achieve the above properties [15]. The degrees of freedom for $\hat{\mathbf{V}}(\hat{E})$ can be chosen to be the values of $\hat{\mathbf{v}}\cdot\hat{\mathbf{n}}_{\hat{e}}$ at any three points on each face $\hat{e}$ [14, 13, 15].

The BDDF_1 spaces on any hexahedral element $E \in \mathcal{T}_h$ are defined via the transformations

$$\mathbf{v} \leftrightarrow \hat{\mathbf{v}} : \mathbf{v} = \frac{1}{J_E} DF_E \hat{\mathbf{v}} \circ F_E^{-1}, \quad w \leftrightarrow \hat{w} : w = \hat{w} \circ F_E^{-1}, \tag{2.12}$$

where the Piola transformation is used for the velocity space. Under this transformation, the normal components of the velocity vectors on the faces are preserved.

Moreover [15],

(2.13)
$$\forall\, \hat{\mathbf{v}} \in \hat{\mathbf{V}}(\hat{E}),\ \forall\, \hat{w} \in \hat{W}(\hat{E}),\ (\nabla \cdot \mathbf{v}, w)_E = (\hat{\nabla} \cdot \hat{\mathbf{v}}, \hat{w})_{\hat{E}},\ \text{and}\ \langle \mathbf{v} \cdot \mathbf{n}_e, w \rangle_e = \langle \hat{\mathbf{v}} \cdot \hat{\mathbf{n}}_{\hat{e}}, \hat{w} \rangle_{\hat{e}}.$$

Note that (2.13) implies, using (2.9),

$$\mathbf{v} \cdot \mathbf{n}_e = \frac{1}{J_e} \hat{\mathbf{v}} \cdot \hat{\mathbf{n}}_{\hat{e}}, \quad \nabla \cdot \mathbf{v} = \left(\frac{1}{J_E} \hat{\nabla} \cdot \hat{\mathbf{v}} \right) \circ F_E^{-1}(\mathbf{x}). \tag{2.14}$$

It is clear that $\nabla \cdot \mathbf{v}|_E \neq$ constant, which leads to certain technical difficulties in the analysis.

The BDDF$_1$ spaces on $\mathcal{T}_h$ are given by

$$\begin{aligned} \mathbf{V}_h &= \{\mathbf{v} \in \mathbf{V}\colon \quad \mathbf{v}|_E \leftrightarrow \hat{\mathbf{v}},\ \hat{\mathbf{v}} \in \hat{\mathbf{V}}(\hat{E}) \quad \forall E \in \mathcal{T}_h\}, \\ W_h &= \{w \in W\colon \quad w|_E \leftrightarrow \hat{w},\ \hat{w} \in \hat{W}(\hat{E}) \quad \forall E \in \mathcal{T}_h\}. \end{aligned} \tag{2.15}$$

In [13], where cubic grids were considered, an MFE projection operator was defined, which here we use as a reference element projection operator. Let $\hat{\Pi} : (H^1(\hat{E}))^3 \to \hat{\mathbf{V}}(\hat{E})$ satisfy

$$\forall\, \hat{e} \subset \partial \hat{E}, \qquad \langle (\hat{\Pi}\hat{\mathbf{q}} - \hat{\mathbf{q}}) \cdot \hat{\mathbf{n}}_{\hat{e}}, \hat{p}_1 \rangle_{\hat{e}} = 0 \qquad \forall\, \hat{p}_1 \in P_1(\hat{e}). \tag{2.16}$$

Using the Piola transformation, we define a projection operator Π from $\mathbf{V} \cap (H^1(\Omega))^3$ onto $\mathbf{V}_h$ satisfying on each element E

$$\Pi\mathbf{q} \leftrightarrow \widehat{\Pi\mathbf{q}}, \quad \widehat{\Pi\mathbf{q}} = \hat{\Pi}\hat{\mathbf{q}}. \tag{2.17}$$

Using (2.14), (2.16), and (2.17), it is easy to see that $\Pi\mathbf{q} \cdot \mathbf{n}$ is continuous across element faces, so it is in $\mathbf{V}_h$, and that it satisfies

$$(\nabla \cdot (\Pi\mathbf{q} - \mathbf{q}), w) = 0 \qquad \forall\, w \in W_h. \tag{2.18}$$

Similarly, one can see that $\Pi\mathbf{q} \cdot \mathbf{n} = 0$ on Γ_N if $\mathbf{q} \cdot \mathbf{n} = 0$ on Γ_N. Details of these arguments can be found in [15, 45, 6, 48].

We will also use the projection operator onto the lowest order RT spaces on hexahedra [44, 38, 37, 15]. The RT$_0$ spaces are defined on the unit cube as

$$\hat{\mathbf{V}}^0(\hat{E}) = \begin{pmatrix} \alpha_1 + \beta_1 \hat{x} \\ \alpha_2 + \beta_2 \hat{y} \\ \alpha_3 + \beta_3 \hat{z} \end{pmatrix}, \quad \hat{W}^0(\hat{E}) = P_0(\hat{E}). \tag{2.19}$$

It holds that $\hat{\nabla} \cdot \hat{\mathbf{V}}^0(\hat{E}) = \hat{W}^0(\hat{E})$ and $\hat{\mathbf{v}} \cdot \hat{\mathbf{n}}_{\hat{e}} \in P_0(\hat{e})$. The degrees of freedom of $\hat{\mathbf{V}}^0(\hat{E})$ are the values of $\hat{\mathbf{v}} \cdot \hat{\mathbf{n}}_{\hat{e}}$ at the midpoints of the six faces. The projection operator $\hat{\Pi}_0 : (H^1(\hat{E}))^3 \to \hat{\mathbf{V}}^0(\hat{E})$ satisfies

$$\forall\, \hat{e} \subset \partial \hat{E}, \qquad \langle (\hat{\Pi}_0\hat{\mathbf{q}} - \hat{\mathbf{q}}) \cdot \hat{\mathbf{n}}_{\hat{e}}, \hat{p}_0 \rangle_{\hat{e}} = 0 \qquad \forall\, \hat{p}_0 \in P_0(\hat{e}). \tag{2.20}$$

The spaces $\mathbf{V}_h^0$ and W_h^0 on $\mathcal{T}_h$ and the projection operator $\Pi_0 : \mathbf{V} \cap (H^1(\Omega))^3 \to \mathbf{V}_h^0$ are defined similarly to the case of BDDF$_1$ spaces. Note that $\mathbf{V}_h^0 \subset \mathbf{V}_h$, $W_h^0 = W_h$,

$$(\nabla \cdot (\Pi_0\mathbf{q} - \mathbf{q}), w) = 0 \qquad \forall\, w \in W_h^0, \tag{2.21}$$

$$\nabla \cdot \mathbf{v} = \nabla \cdot \Pi_0\mathbf{v} \quad \forall\, \mathbf{v} \in \mathbf{V}_h, \tag{2.22}$$

and

$$\|\Pi_0\mathbf{v}\| \leq C\|\mathbf{v}\| \quad \forall\, \mathbf{v} \in \mathbf{V}_h. \tag{2.23}$$

2.3.1. An enhanced BDDF$_1$ space. The MPFA elimination procedure requires on each face one velocity degree of freedom to be associated with each vertex. Since the BDDF$_1$ space $\mathbf{V}_h$ has only three degrees of freedom per face, we need to augment it with six more degrees of freedom. In doing so, we need to preserve the constant divergence, so we add six more curl terms. These terms should also preserve the linear independence of the shape functions and the continuity of the normal component across element faces. As in the definition of the original BDDF$_1$ space, there is more than one way to achieve this. We define

(2.24)
$$\begin{aligned}\hat{\mathbf{V}}^*(\hat{E}) &= \hat{\mathbf{V}}(\hat{E}) + r_2\ \mathrm{curl}(0,0,\hat{x}^2\hat{z})^T + r_3\ \mathrm{curl}(0,0,\hat{x}^2\hat{y}\hat{z})^T + s_2\ \mathrm{curl}(\hat{x}\hat{y}^2,0,0)^T\\ &\quad + s_3\ \mathrm{curl}(\hat{x}\hat{y}^2\hat{z},0,0)^T + t_2\ \mathrm{curl}(0,\hat{y}\hat{z}^2,0)^T + t_3\ \mathrm{curl}(0,\hat{x}\hat{y}\hat{z}^2,0)^T\\ &= \hat{\mathbf{V}}(\hat{E}) + r_2(0,-2\hat{x}\hat{z},0)^T + r_3(\hat{x}^2\hat{z},-2\hat{x}\hat{y}\hat{z},0)^T + s_2(0,0,-2\hat{x}\hat{y})^T\\ &\quad + s_3(0,\hat{x}\hat{y}^2,-2\hat{x}\hat{y}\hat{z})^T + t_2(-2\hat{y}\hat{z},0,0)^T + t_3(-2\hat{x}\hat{y}\hat{z},0,\hat{y}\hat{z}^2),\\ \hat{W}(\hat{E}) &= P_0(\hat{E}).\end{aligned}$$

We have

$$\hat{\nabla}\cdot\hat{\mathbf{V}}^*(\hat{E}) = \hat{W}(\hat{E}) \quad \text{and} \quad \forall\,\hat{\mathbf{v}}\in\hat{\mathbf{V}}^*(\hat{E}),\ \forall\,\hat{e}\subset\partial\hat{E},\ \hat{\mathbf{v}}\cdot\hat{\mathbf{n}}_{\hat{e}}\in Q_1(\hat{e}), \tag{2.25}$$

where Q_1 is the space of bilinear functions.

LEMMA 2.1. *The dimension of* $\hat{\mathbf{V}}^*(\hat{E})$ *is* 24.

Proof. It is enough to show that the 12 vectors added to $P_1(\hat{E})^3$ in definitions (2.11) and (2.24) are linearly independent. Denote these vectors by $\mathbf{v}_i$, $i=1,\dots,12$, and assume that $\sum_{i=1}^{12}\alpha_i\mathbf{v}_i = 0$. The first component of this equation implies that $\alpha_1=\alpha_6=\alpha_8=\alpha_{11}=\alpha_{12}=0$. The second component implies that $\alpha_2=\alpha_3=\alpha_4=\alpha_7=\alpha_{10}=0$. The third component implies that $\alpha_5=\alpha_9=0$. ∎

The following lemma establishes degrees of freedom for $\hat{\mathbf{V}}^*(\hat{E})$.

LEMMA 2.2. *Any vector* $\hat{\mathbf{v}}\in\hat{\mathbf{V}}^*(\hat{E})$ *is uniquely determined by the moments*

$$\forall\,\hat{e}\subset\partial\hat{E},\quad \langle\hat{\mathbf{v}}\cdot\hat{\mathbf{n}}_{\hat{e}},\hat{p}_1\rangle_{\hat{e}},\quad \hat{p}_1\in Q_1(\hat{e}). \tag{2.26}$$

Proof. Let $\hat{\mathbf{v}}\in\hat{\mathbf{V}}^*(\hat{E})$. Using (2.11) and (2.24), the three components of $\hat{\mathbf{v}}$ are

$$\begin{aligned}\hat{v}_1 &= p_1(\hat{x},\hat{y},\hat{z}) + r_0\hat{x}\hat{z} + 2r_1\hat{x}\hat{y} - t_0\hat{x}\hat{y} - t_1\hat{x}^2 + r_3\hat{x}^2\hat{z} - 2t_2\hat{y}\hat{z} - 2t_3\hat{x}\hat{y}\hat{z},\\ \hat{v}_2 &= p_2(\hat{x},\hat{y},\hat{z}) - r_0\hat{y}\hat{z} - r_1\hat{y}^2 + s_0\hat{x}\hat{y} + 2s_1\hat{y}\hat{z} - 2r_2\hat{x}\hat{z} - 2r_3\hat{x}\hat{y}\hat{z} + s_3\hat{x}\hat{y}^2,\\ \hat{v}_3 &= p_3(\hat{x},\hat{y},\hat{z}) - s_0\hat{x}\hat{z} - s_1\hat{z}^2 + t_0\hat{y}\hat{z} + 2t_1\hat{x}\hat{z} - 2s_2\hat{x}\hat{y} - 2s_3\hat{x}\hat{y}\hat{z} + t_3\hat{y}\hat{z}^2,\end{aligned}$$

where $p_i(\hat{x},\hat{y},\hat{z}) = a_i\hat{x}+b_i\hat{y}+c_i\hat{z}+d_i$, $i=1,2,3$. Let us assume that all moments (2.26) are zero. Since $\hat{\mathbf{v}}\cdot\hat{\mathbf{n}}_{\hat{e}}\in Q_1(\hat{e})$, we conclude that $\hat{\mathbf{v}}\cdot\hat{\mathbf{n}}_{\hat{e}}=0$ for all faces $\hat{e}$. For the face $\hat{x}=0$ we have $\hat{v}_1=0$, which implies $b_1=c_1=d_1=t_2=0$. For the face $\hat{x}=1$ we also have $\hat{v}_1=0$, which implies $a_1-t_1=0$, $2r_1-t_0=0$, $r_0+r_3=0$, and $t_3=0$. Similarly, $\hat{v}_2=0$ at $\hat{y}=0$, implying $a_2=c_2=d_2=r_2=0$, and $\hat{v}_2=0$ at $\hat{y}=1$, implying $b_2-r_1=0$, $s_0+s_3=0$, $-r_0+2s_1=0$, and $r_3=0$. Finally, $\hat{v}_3=0$ at $\hat{z}=0$ implies $a_3=b_3=d_3=s_2=0$, and $\hat{v}_3=0$ at $\hat{z}=1$ implies $c_1-s_1=0$, $-s_0+2t_1=0$, $t_0+t_3=0$, and $s_3=0$. It is easy to see that the above equations imply $a_i=b_i=c_i=d_i=0$, $i=1,2,3$, and $r_i=s_i=t_i=0$, $i=0,1,2,3$; hence $\hat{\mathbf{v}}=0$. ∎

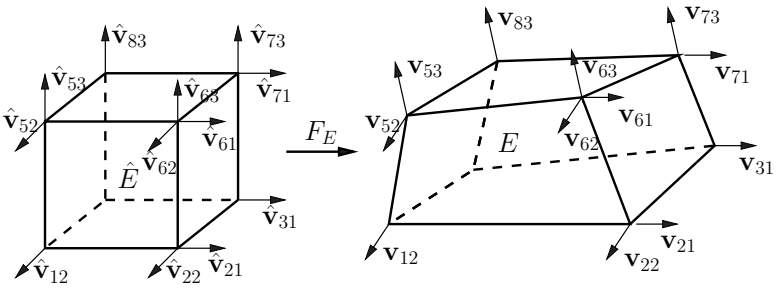

FIG. 2. *Degrees of freedom and basis functions for the enhanced BDDF$_1$ velocity space on hexahedra.*

Since $\dim Q_1(\hat{e}) = 4$, the number of moments in (2.26) is 24, equal to $\dim \hat{\mathbf{V}}^*(\hat{E})$. Therefore these moments can be used to define the degrees of freedom of $\hat{\mathbf{V}}^*(\hat{E})$. In particular, these can be the values of $\hat{\mathbf{v}} \cdot \hat{\mathbf{n}}_{\hat{e}}$ at four different points (such that no three points are colinear) on each of the six faces. We choose these points to be the vertices of $\hat{e}$; see Figure 2. This choice gives certain orthogonalities for the quadrature rule introduced in the next section.

Lemma 2.2 implies that there exists a unique projection operator $\hat{\Pi}_* : (H^1(\hat{E}))^3 \to \hat{\mathbf{V}}^*(\hat{E})$ such that

$$\forall\, \hat{e} \subset \partial \hat{E}, \qquad \langle (\hat{\Pi}_* \hat{\mathbf{q}} - \hat{\mathbf{q}}) \cdot \hat{\mathbf{n}}_{\hat{e}}, \hat{p}_1 \rangle_{\hat{e}} = 0 \qquad \forall\, \hat{p}_1 \in Q_1(\hat{e}). \tag{2.27}$$

The divergence theorem and (2.27) imply that

$$(\hat{\nabla} \cdot (\hat{\Pi}_* \hat{\mathbf{q}} - \hat{\mathbf{q}}), \hat{w})_{\hat{E}} = 0 \qquad \forall\, \hat{w} \in \hat{W}(\hat{E}). \tag{2.28}$$

The enhanced BDDF$_1$ spaces $\mathbf{V}_h^* \times W_h$ on $\mathcal{T}_h$ are defined as in (2.15). The projection operator Π_* from $\mathbf{V} \cap (H^1(\Omega))^3$ onto $\mathbf{V}_h^*$ is defined via the Piola transformation, as in (2.17).

LEMMA 2.3. *The projection operator Π_* defined by* (2.27) *and* (2.17) *is an operator from $\mathbf{V} \cap (H^1(\Omega))^3$ onto $\mathbf{V}_h^*$. Moreover,*

$$(\nabla \cdot (\Pi_* \mathbf{q} - \mathbf{q}), w) = 0 \qquad \forall\, w \in W_h. \tag{2.29}$$

Proof. Let $\mathbf{q} \in (H^1(\Omega))^3$. To prove that $\Pi_* \mathbf{q} \in H(\mathrm{div}; \Omega)$, we need to show that $\Pi_* \mathbf{q} \cdot \mathbf{n}$ is continuous across element faces.

First, note that (2.25) and (2.14) imply that on any face e

$$\Pi_* \mathbf{q} \cdot \mathbf{n}_e \in \frac{1}{J_e} Q_1(\hat{e}) \circ F^{-1}(\mathbf{x}). \tag{2.30}$$

Let e be a face shared by elements E_1 and E_2. Let $\mathbf{n}_e^{E_i}$ be the outward unit normal to ∂E_i on e. Let $\hat{e}_i$ be the face of $\hat{E}$ corresponding to e in the mapping $F_{E_i} : \hat{E} \to E_i$. Using (2.13), (2.17), and (2.27), we have, for all $p_1 \in Q_1(\hat{e}) \circ F^{-1}(\mathbf{x})$,

$$\langle \Pi_* \mathbf{q}_{E_i} \cdot \mathbf{n}_e^{E_i}, p_1 \rangle_e = \langle \widehat{\Pi_* \mathbf{q}}_{E_i} \cdot \hat{\mathbf{n}}_{\hat{e}_i}, \hat{p}_1 \rangle_{\hat{e}_i} = \langle \hat{\Pi}_* \hat{\mathbf{q}}_{E_i} \cdot \hat{\mathbf{n}}_{\hat{e}_i}, \hat{p}_1 \rangle_{\hat{e}_i} = \langle \hat{\mathbf{q}}_{E_i} \cdot \hat{\mathbf{n}}_{\hat{e}_i}, \hat{p}_1 \rangle_{\hat{e}_i}.$$

Since $\hat{\mathbf{q}}_{E_1}|_{\hat{e}_1} = \hat{\mathbf{q}}_{E_2}|_{\hat{e}_2}$ and $\hat{\mathbf{n}}_{\hat{e}_1} = -\hat{\mathbf{n}}_{\hat{e}_2}$, the above equation and (2.30) imply that

$$\Pi_* \mathbf{q}_{E_1} \cdot \mathbf{n}_e^{E_1} + \Pi_* \mathbf{q}_{E_2} \cdot \mathbf{n}_e^{E_2} = 0;$$

therefore $\Pi_* \mathbf{q} \in H(\mathrm{div}; \Omega)$. A similar argument shows that if $\mathbf{q} \cdot \mathbf{n} = 0$ on Γ_N, then $\Pi_* \mathbf{q} \cdot \mathbf{n} = 0$ on Γ_N.

Finally, (2.29) follows from (2.28) and (2.13). ∎

2.4. A quadrature rule. The integration on any element E is performed by mapping to the reference element $\hat{E}$. The quadrature rule is defined on $\hat{E}$. Using the definition (2.12), (2.15) of the finite element spaces we have for $\mathbf{q}$, $\mathbf{v} \in \mathbf{V}_h^*$,

$$\begin{aligned}\int_E K^{-1}\mathbf{q}\cdot\mathbf{v}\,\mathrm{d}\mathbf{x} &= \int_{\hat{E}} \hat{K}^{-1}\frac{1}{J_E}DF_E\hat{\mathbf{q}}\cdot\frac{1}{J_E}DF_E\hat{\mathbf{v}}\,J_E\,\mathrm{d}\hat{\mathbf{x}}\\ &= \int_{\hat{E}}\frac{1}{J_E}DF_E^T\hat{K}^{-1}DF_E\,\hat{\mathbf{q}}\cdot\hat{\mathbf{v}}\,\mathrm{d}\hat{\mathbf{x}} \equiv \int_{\hat{E}}\mathcal{K}^{-1}\hat{\mathbf{q}}\cdot\hat{\mathbf{v}}\,\mathrm{d}\hat{\mathbf{x}},\end{aligned}$$

where

$$\mathcal{K} = J_E DF_E^{-1}\hat{K}(DF_E^{-1})^T. \tag{2.31}$$

It is easy to see that (2.10) and (2.5) imply that

$$\|\mathcal{K}\|_{0,\infty,\hat{E}} \sim h\|K\|_{0,\infty,E}, \quad \|\mathcal{K}^{-1}\|_{0,\infty,\hat{E}} \sim h^{-1}\|K^{-1}\|_{0,\infty,E}, \tag{2.32}$$

and

$$c_0k_0h\,\xi^T\xi \le \xi^T\mathcal{K}(\hat{\mathbf{x}})\xi \le c_1k_1h\,\xi^T\xi \quad \forall\hat{\mathbf{x}}\in\hat{E}\ \forall\xi\in\mathbb{R}^3, \tag{2.33}$$

where the notation $a \sim b$ means that there exist positive constants c_0 and c_1 independent of h such that $c_0b \le a \le c_1b$. The quadrature rule on an element E is defined as

$$(K^{-1}\mathbf{q},\mathbf{v})_{Q,E} \equiv (\mathcal{K}^{-1}\hat{\mathbf{q}},\hat{\mathbf{v}})_{\hat{Q},\hat{E}} \equiv \frac{|\hat{E}|}{8}\sum_{i=1}^{8}\mathcal{K}^{-1}(\hat{\mathbf{r}}_i)\hat{\mathbf{q}}(\hat{\mathbf{r}}_i)\cdot\hat{\mathbf{v}}(\hat{\mathbf{r}}_i), \tag{2.34}$$

which is the trapezoidal quadrature rule on $\hat{E}$. The global quadrature rule is defined as

$$(K^{-1}\mathbf{q},\mathbf{v})_Q \equiv \sum_{E\in\mathcal{T}_h}(K^{-1}\mathbf{q},\mathbf{v})_{Q,E}.$$

The corner vector $\hat{\mathbf{q}}(\hat{\mathbf{r}}_i)$ is uniquely determined by its normal components to the three faces that share that vertex. Since we chose the velocity degrees of freedom on any face $\hat{e}$ to be the normal components at the vertices of $\hat{e}$, there are three degrees of freedom associated with each corner $\hat{\mathbf{r}}_i$, and they uniquely determine the corner vector $\hat{\mathbf{q}}(\hat{\mathbf{r}}_i)$. More precisely,

$$\hat{\mathbf{q}}(\hat{\mathbf{r}}_i) = \sum_{j=1}^{3}(\hat{\mathbf{q}}\cdot\hat{\mathbf{n}}_{ij})(\hat{\mathbf{r}}_i)\hat{\mathbf{n}}_{ij},$$

where $\hat{\mathbf{n}}_{ij}$, $j = 1,\dots,3$, are the outward unit normal vectors to the three faces sharing $\hat{\mathbf{r}}_i$, and $(\hat{\mathbf{q}}\cdot\hat{\mathbf{n}}_{ij})(\hat{\mathbf{r}}_i)$ are the velocity degrees of freedom associated with this corner. Denote the basis functions associated with $\hat{\mathbf{r}}_i$ by $\hat{\mathbf{v}}_{ij}$, $j = 1,\dots,3$ (see Figure 2), i.e.,

$$(\hat{\mathbf{v}}_{ij}\cdot\hat{\mathbf{n}}_{ij})(\hat{\mathbf{r}}_i) = 1,\ \ (\hat{\mathbf{v}}_{ij}\cdot\hat{\mathbf{n}}_{ik})(\hat{\mathbf{r}}_i) = 0,\ k\ne j,\ \text{and}\ (\hat{\mathbf{v}}_{ij}\cdot\hat{\mathbf{n}}_{lk})(\hat{\mathbf{r}}_l) = 0,\ l\ne i,\ k = 1,\dots,3.$$

The quadrature rule (2.34) couples only the three basis functions associated with a corner. For example,

$$\begin{aligned}&(\mathcal{K}^{-1}\hat{\mathbf{v}}_{11},\hat{\mathbf{v}}_{11})_{\hat{Q},\hat{E}} = \frac{\mathcal{K}_{11}^{-1}(\hat{\mathbf{r}}_1)}{8}, \quad (\mathcal{K}^{-1}\hat{\mathbf{v}}_{11},\hat{\mathbf{v}}_{12})_{\hat{Q},\hat{E}} = \frac{\mathcal{K}_{21}^{-1}(\hat{\mathbf{r}}_1)}{8},\\ &(\mathcal{K}^{-1}\hat{\mathbf{v}}_{11},\hat{\mathbf{v}}_{13})_{\hat{Q},\hat{E}} = \frac{\mathcal{K}_{31}^{-1}(\hat{\mathbf{r}}_1)}{8}, \quad \text{and} \quad (\mathcal{K}^{-1}\hat{\mathbf{v}}_{11},\hat{\mathbf{v}}_{ij})_{\hat{Q},\hat{E}} = 0 \quad \forall\, ij \ne 11,12,13.\end{aligned} \tag{2.35}$$

Using (2.12) and (2.31), (2.34) implies

$$(K^{-1}\mathbf{q},\mathbf{v})_{Q,E} = \frac{1}{8}\sum_{i=1}^{8} K^{-1}(\mathbf{r}_i) J_E(\hat{\mathbf{r}}_i)\mathbf{q}(\mathbf{r}_i)\cdot\mathbf{v}(\mathbf{r}_i), \tag{2.36}$$

which is related to an inner product used in the MFD methods [28, 35].

Denote the element quadrature error by

$$\sigma_E(K^{-1}\mathbf{q},\mathbf{v}) \equiv (K^{-1}\mathbf{q},\mathbf{v})_E - (K^{-1}\mathbf{q},\mathbf{v})_{Q,E}, \tag{2.37}$$

and define the global quadrature error by $\sigma(K^{-1}\mathbf{q},\mathbf{v})|_E = \sigma_E(K^{-1}\mathbf{q},\mathbf{v})$. Similarly, denote the quadrature error on the reference element by

$$\hat{\sigma}_{\hat{E}}(\mathcal{K}^{-1}\hat{\mathbf{q}},\hat{\mathbf{v}}) \equiv (\mathcal{K}^{-1}\hat{\mathbf{q}},\hat{\mathbf{v}})_{\hat{E}} - (\mathcal{K}^{-1}\hat{\mathbf{q}},\hat{\mathbf{v}})_{\hat{Q},\hat{E}}. \tag{2.38}$$

The following lemma will be used to bound the quadrature error.

LEMMA 2.4. *For any* $\hat{\mathbf{q}} \in \hat{\mathbf{V}}^*(\hat{E})$,

$$(\hat{\mathbf{q}} - \hat{\Pi}_0\hat{\mathbf{q}},\hat{\mathbf{v}}_0)_{\hat{Q},\hat{E}} = 0 \quad \textit{for all constant vectors } \hat{\mathbf{v}}_0. \tag{2.39}$$

Proof. On any face $\hat{e}$, if the degrees of freedom of $\hat{\mathbf{q}}$ are $\hat{q}_{\hat{e},i}$, $i = 1,\dots,4$, then (2.20) and an application of the trapezoidal quadrature rule imply that $\hat{\Pi}_0\hat{\mathbf{q}}\cdot\hat{\mathbf{n}}_{\hat{e}} = (\hat{q}_{\hat{e},1}+\hat{q}_{\hat{e},2}+\hat{q}_{\hat{e},3}+\hat{q}_{\hat{e},4})/4$. The assertion of the lemma follows from a simple calculation, using (2.34). ∎

2.5. The MFMFE method. Let $\mathcal{P}_0 : L^2(\partial\Omega) \to \mathbf{V}_h^0\cdot\mathbf{n}$ be the L^2-orthogonal projection onto the space of piecewise constant functions on the trace of $\mathcal{T}_h$ on $\partial\Omega$:

$$\forall\varphi \in L^2(\Omega), \quad \langle\varphi - \mathcal{P}_0\varphi, \mathbf{v}\cdot\mathbf{n}\rangle_{\partial\Omega} = 0 \ \forall\mathbf{v} \in \mathbf{V}_h^0. \tag{2.40}$$

In the method defined below, the Dirichlet boundary data g is incorporated into the scheme as $\mathcal{P}_0 g$. As we see in the analysis, this is necessary for optimal approximation of the boundary condition term.

The method is defined as follows: find $\mathbf{u}_h \in \mathbf{V}_h^*$ and $p_h \in W_h$ such that

$$(K^{-1}\mathbf{u}_h,\mathbf{v})_Q = (p_h,\nabla\cdot\mathbf{v}) - \langle\mathcal{P}_0 g,\mathbf{v}\cdot\mathbf{n}\rangle_{\Gamma_D}, \quad \mathbf{v} \in \mathbf{V}_h^*, \tag{2.41}$$

$$(\nabla\cdot\mathbf{u}_h, w) = (f,w), \quad w \in W_h. \tag{2.42}$$

Following the terminology from [48], we call the method (2.41)–(2.42) an MFMFE method, due to its relation to the MPFA method.

Before we prove existence and uniqueness of a solution to (2.41)–(2.42), we show that the quadrature rule (2.34) produces a coercive bilinear form. We have the following auxiliary result.

LEMMA 2.5. *If* $E \in \mathcal{T}_h$ *and* $\mathbf{q} \in (L^2(E))^3$, *then*

$$\|\mathbf{q}\|_E \sim h^{-\frac{1}{2}}\|\hat{\mathbf{q}}\|_{\hat{E}}. \tag{2.43}$$

Proof. Using (2.12), we have

$$\int_E \mathbf{q}\cdot\mathbf{q}\,\mathrm{d}\mathbf{x} = \int_{\hat{E}} \frac{1}{J_E} DF_E\hat{\mathbf{q}}\cdot\frac{1}{J_E} DF_E\hat{\mathbf{q}}\, J_E\,\mathrm{d}\hat{\mathbf{x}}$$

and

$$\int_{\hat{E}} \hat{\mathbf{q}} \cdot \hat{\mathbf{q}} \, \mathrm{d}\hat{\mathbf{x}} = \int_E \frac{1}{J_{F_E^{-1}}} DF_E^{-1}\mathbf{q} \cdot \frac{1}{J_{F_E^{-1}}} DF_E^{-1}\mathbf{q} J_{F_E^{-1}} \, \mathrm{d}\mathbf{x}.$$

The result follows from the bounds (2.10). ∎

Let $\mathbf{P}_h^0$ be the space of piecewise constant vectors on $\mathcal{T}_h$ and let $\bar{\mathbf{V}}_h^* = \mathbf{V}_h^* \bigoplus \mathbf{P}_h^0$.

LEMMA 2.6. *The bilinear form* $(K^{-1}\mathbf{q}, \mathbf{v})_Q$ *is an inner product in* $\bar{\mathbf{V}}_h^*$. *Furthermore,* $(K^{-1}\mathbf{q}, \mathbf{q})_Q^{1/2}$ *is a norm in* $\bar{\mathbf{V}}_h^*$ *equivalent to* $\|\cdot\|$.

Proof. Let $\mathbf{q}$, $\mathbf{v} \in \bar{\mathbf{V}}_h^*$. Clearly $(K^{-1}\mathbf{q}, \mathbf{v})_Q$ is linear and symmetric. It is easy to check that

$$\frac{|\hat{E}|}{8} \sum_{i=1}^{8} \hat{\mathbf{q}}(\hat{\mathbf{r}}_i) \cdot \hat{\mathbf{q}}(\hat{\mathbf{r}}_i) \sim \|\hat{\mathbf{q}}\|_{\hat{E}}^2. \tag{2.44}$$

Combining (2.34), (2.33), (2.44), and (2.43), we conclude that

$$(K^{-1}\mathbf{q}, \mathbf{q})_{Q,E} \sim \|\mathbf{q}\|_E^2, \tag{2.45}$$

which implies the assertion of the lemma. ∎

We continue with the solvability of the method (2.41)–(2.42).

LEMMA 2.7. *The MFMFE method* (2.41)–(2.42) *has a unique solution.*

Proof. Since (2.41)–(2.42) is a square system, it is enough to show uniqueness. Let $f = 0$, $g = 0$, and take $\mathbf{v} = \mathbf{u}_h$ and $w = p_h$. This implies that $(K^{-1}\mathbf{u}_h, \mathbf{u}_h)_Q = 0$, and therefore $\mathbf{u}_h = 0$, due to (2.45). We now consider the auxiliary problem

$$\nabla \cdot \boldsymbol{\psi} = p_h \ \text{ in } \Omega, \quad \boldsymbol{\psi} = \mathbf{g}_1 \ \text{ on } \partial\Omega, \tag{2.46}$$

where $\mathbf{g}_1 \in (H^{1/2}(\partial\Omega))^3$ is constructed to satisfy $\int_{\partial\Omega} \mathbf{g}_1 \cdot \mathbf{n} = \int_\Omega p_h$ and $\mathbf{g}_1 \cdot \mathbf{n} = 0$ on Γ_N. More precisely, we take $\mathbf{g}_1 = (\int_\Omega p_h)\varphi\mathbf{n}$, where $\varphi \in C^0(\partial\Omega)$ is such that $\int_{\partial\Omega} \varphi = 1$ and $\varphi = 0$ on Γ_N. Clearly $\|\mathbf{g}_1\|_{1/2,\partial\Omega} \le C\|p_h\|$. It is known [25] that the above problem has a solution satisfying

$$\|\boldsymbol{\psi}\|_1 \le C(\|p_h\| + \|\mathbf{g}_1\|_{1/2,\partial\Omega}) \le C\|p_h\|. \tag{2.47}$$

The regularity of $\boldsymbol{\psi}$ guarantees that $\Pi^*\boldsymbol{\psi}$ is well defined. The choice $\mathbf{v} = \Pi_*\boldsymbol{\psi} \in \mathbf{V}_h^*$ in (2.41) gives

$$0 = (p_h, \nabla \cdot \Pi_*\boldsymbol{\psi}) = (p_h, \nabla \cdot \boldsymbol{\psi}) = \|p_h\|^2;$$

therefore $p_h = 0$. ∎

2.6. Reduction to a cell-centered stencil. In this section we describe how the MFMFE method reduces to a system for the pressures at the cell centers. Any interior vertex $\mathbf{r}$ is shared by eight elements $E_1, \ldots, E_8$; see Figure 3 (the lower back left element E_4 and the upper front right element E_6 are not labeled to avoid cluttering the image). We denote the faces that share the vertex by $e_1, \ldots, e_{12}$, and the velocity basis functions on these faces that are associated with the vertex by $\mathbf{v}_1, \ldots, \mathbf{v}_{12}$, i.e., $(\mathbf{v}_i \cdot \mathbf{n}_i)(\mathbf{r}) = 1$, where $\mathbf{n}_i$ is the unit normal on face e_i. Let the corresponding values of the normal components of $\mathbf{u}_h$ be $u_1, \ldots, u_{12}$. Note that for clarity the normal velocities on Figure 3 are drawn at a distance from the vertex. The three images depict the normal velocities in directions x, y, and z, respectively.

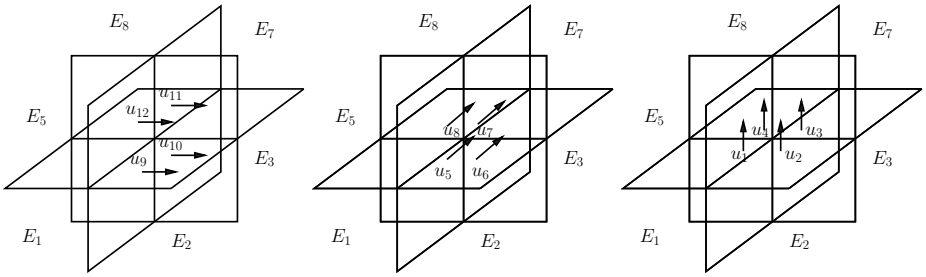

FIG. 3. *Interactions of the velocity degrees of freedom in the MFMFE method.*

Since the quadrature rule $(K^{-1}\cdot,\cdot)_Q$ localizes the basis functions interaction (see (2.35)), taking $\mathbf{v} = \mathbf{v}_1$ in (2.41), for example, will lead to coupling u_1 only with u_5, u_8, u_9, and u_{12}. Similarly, u_2 will be coupled only with u_6, u_7, u_9, and u_{12}, etc. Therefore, the 12 equations obtained from taking $\mathbf{v} = \mathbf{v}_1, \ldots, \mathbf{v}_{12}$ form a linear system for $u_1, \ldots, u_{12}$.

PROPOSITION 2.1. *The* 12×12 *local linear system described above is symmetric and positive definite.*

Proof. The system is obtained by taking $\mathbf{v} = \mathbf{v}_1, \ldots, \mathbf{v}_{12}$ in (2.41). On the left-hand side we have

$$(K^{-1}\mathbf{u}_h, \mathbf{v}_i)_Q = \sum_{j=1}^{12} u_j (K^{-1}\mathbf{v}_j, \mathbf{v}_i)_Q \equiv \sum_{j=1}^{k} a_{ij} u_j, \quad i = 1, \ldots, 12.$$

Using Lemma 2.6 we conclude that the matrix $\bar{A} = \{a_{ij}\}$ is symmetric and positive definite. ∎

We use the notation in the example in Figure 3 to describe the local linear system. For example, taking $\mathbf{v} = \mathbf{v}_9$ in (2.41), we obtain on the left-hand side of the equation

$$(K^{-1}\mathbf{u}_h, \mathbf{v}_9)_Q = (K^{-1}\mathbf{u}_h, \mathbf{v}_9)_{Q,E_1} + (K^{-1}\mathbf{u}_h, \mathbf{v}_9)_{Q,E_2}. \tag{2.48}$$

Using (2.34), the first term on the right above gives

$$\begin{aligned}(K^{-1}\mathbf{u}_h, \mathbf{v}_9)_{Q,E_1} &= (\mathcal{K}^{-1}\hat{\mathbf{u}}_h, \hat{\mathbf{v}}_9)_{\hat{Q},\hat{E}} \\ &= \sum_i u_i (\mathcal{K}^{-1}\hat{\mathbf{v}}_i, \hat{\mathbf{v}}_9)_{\hat{Q},\hat{E}} \\ &= \frac{1}{8}(\mathcal{K}^{-1}_{11,E_1}|e_9|u_9 + \mathcal{K}^{-1}_{12,E_1}|e_5|u_5 + \mathcal{K}^{-1}_{13,E_1}|e_1|u_1)|e_9|,\end{aligned} \tag{2.49}$$

where we have used (2.14) for the last equality and $\mathcal{K}^{-1}_{ij,E_1}$ denotes a component of $\mathcal{K}^{-1}$ in E_1 evaluated at the vertex of $\hat{E}$ corresponding to vertex $\mathbf{r}$ in the mapping F_{E_1}. Similarly, the second term in (2.48) is

$$(K^{-1}\mathbf{u}_h, \mathbf{v}_9)_{Q,E_2} = \frac{1}{8}(\mathcal{K}^{-1}_{11,E_2}|e_9|u_9 + \mathcal{K}^{-1}_{12,E_2}|e_6|u_6 + \mathcal{K}^{-1}_{13,E_2}|e_2|u_2)|e_9|. \tag{2.50}$$

For the right-hand side of (2.41) we write

$$\begin{aligned}(p_h, \nabla\cdot\mathbf{v}_9) &= (p_h, \nabla\cdot\mathbf{v}_9)_{E_1} + (p_h, \nabla\cdot\mathbf{v}_9)_{E_2} \\ &= \langle p_h, \mathbf{v}_9\cdot\mathbf{n}_{E_1}\rangle_{e_9} + \langle p_h, \mathbf{v}_9\cdot\mathbf{n}_{E_2}\rangle_{e_9} \\ &= \langle \hat{p}_h, \hat{\mathbf{v}}_9\cdot\hat{\mathbf{n}}_{E_1}\rangle_{\hat{e}_9} + \langle \hat{p}_h, \hat{\mathbf{v}}_9\cdot\hat{\mathbf{n}}_{E_2}\rangle_{\hat{e}_9} \\ &= \frac{1}{4}(p_1 - p_2)|e_9|.\end{aligned} \tag{2.51}$$

For the last equality we used the trapezoidal rule for the integrals on $\hat{e}_9$, which is exact since $\hat{p}_h$ is constant and $\hat{\mathbf{v}}_9 \cdot \hat{\mathbf{n}}$ is bilinear. Combining (2.48)–(2.51), we obtain

$$\left(\frac{1}{2}\mathcal{K}^{-1}_{11,E_1} + \frac{1}{2}\mathcal{K}^{-1}_{11,E_2}\right)|e_9|u_9 + \frac{1}{2}\mathcal{K}^{-1}_{12,E_1}|e_5|u_5 + \frac{1}{2}\mathcal{K}^{-1}_{12,E_2}|e_6|u_6 + \frac{1}{2}\mathcal{K}^{-1}_{13,E_1}|e_1|u_1 + \frac{1}{2}\mathcal{K}^{-1}_{13,E_2}|e_2|u_2 = p_1 - p_2.$$

The other 11 equations of the local system for $u_1, \ldots, u_{12}$ are obtained similarly.

The solution of the local 12×12 linear system allows for the velocities u_i, $i = 1, \ldots, 12$, to be expressed in terms of the cell-centered pressures p_i, $i = 1, \ldots, 8$. Substituting these expressions into the mass conservation equation (2.42) leads to a cell-centered stencil. The pressure in each element E is coupled with the pressures in the elements that share a vertex with E; i.e., we obtain a 27 point stencil.

For any vertex on the boundary $\partial\Omega$, the size of the local linear system equals the number of non-Neumann (interior or Dirichlet) faces that share that vertex. In that case solving the local system leads to an expression of the velocities in terms of the element pressures and the boundary data.

We have the following important property of the CCFD algebraic system.

PROPOSITION 2.2. *The CCFD system for the pressure obtained from* (2.41)–(2.42) *using the procedure described above is symmetric and positive definite.*

Proof. The proof follows the argument from Proposition 2.8 in [48]. We present it here for completeness. Denote the bases of $\mathbf{V}_h^*$ and W_h by $\{\mathbf{v}_i\}$ and $\{w_j\}$, respectively. The algebraic system arising from (2.41)–(2.42) is of the saddle point form

$$\begin{pmatrix} A & B^T \\ B & 0 \end{pmatrix}\begin{pmatrix} U \\ P \end{pmatrix} = \begin{pmatrix} G \\ F \end{pmatrix}, \tag{2.52}$$

where $A_{ij} = (K^{-1}\mathbf{v}_i, \mathbf{v}_j)_Q$ and $B_{ij} = -(\nabla \cdot \mathbf{v}_i, w_j)$. The matrix A is symmetric and positive definite, as it is block-diagonal with symmetric and positive definite blocks; see Proposition 2.1. The elimination of U leads to a CCFD system for P with a symmetric and positive semidefinite matrix $BA^{-1}B^T$. It is clear from the proof of Lemma 2.7 that $B^TP = 0$ implies $P = 0$. Therefore $BA^{-1}B^T$ is positive definite. ∎

3. Velocity error analysis.

3.1. Auxiliary estimates. For the convergence analysis we need to impose a restriction on the element geometry. This is due to the reduced approximation properties of the MFE spaces on general hexahedra, as shown below. The numerical experiments in section 5 confirm that the deterioration of convergence on rough grids is not just a theoretical artifact. This is similar to the behavior observed on general quadrilaterals [48, 3].

Recall that since the mapping F_E is trilinear, the faces of an element E may be non-planar. We will refer to the faces as *generalized quadrilaterals*.

DEFINITION 3.1. *A generalized quadrilateral with vertices* $\mathbf{r}_1, \ldots, \mathbf{r}_4$ *is called an* h^2-parallelogram *if*

$$\|\mathbf{r}_{34} - \mathbf{r}_{21}\|_{\mathbb{R}^3} \le Ch^2,$$

where $\|\cdot\|_{\mathbb{R}^3}$ *is the Euclidean vector norm in* $\mathbb{R}^3$.

In the above we assume that the vertices are numbered consecutively along the boundary, which implies that $\mathbf{r}_{34}$ and $\mathbf{r}_{21}$ are opposite sides.

DEFINITION 3.2. *A hexahedral element is called an h^2-parallelepiped if all of its faces are h^2-parallelograms.*

It is clear from (2.8) that the above condition implies that $\frac{\partial^2 F_E}{\partial\hat{x}\partial\hat{y}}$, $\frac{\partial^2 F_E}{\partial\hat{x}\partial\hat{z}}$, and $\frac{\partial^2 F_E}{\partial\hat{y}\partial\hat{z}}$ are $O(h^2)$.

DEFINITION 3.3. *An h^2-parallelepiped is called* regular *if*

$$\|(\mathbf{r}_{21}-\mathbf{r}_{34})-(\mathbf{r}_{65}-\mathbf{r}_{78})\| \le Ch^3.$$

The above condition implies that $\frac{\partial^3 F_E}{\partial\hat{x}\partial\hat{y}\partial\hat{z}}$ is $O(h^3)$.

We have the following bounds on the derivatives of the mapping F_E.

LEMMA 3.1. *The bounds*

(3.1)
$$|DF_E|_{j,\infty,\hat{E}} \le Ch^{j+1}, \quad \left|\frac{1}{J_E}DF_E\right|_{j,\infty,\hat{E}} \le Ch^{j-2}, \quad \text{and} \quad |J_E DF_E^{-1}|_{j,\infty,\hat{E}} \le Ch^{j+2}$$

hold for $j=0$ if E is a general hexahedron, for $j=0,1$ if E is an h^2-parallelepiped, and for $j=0,1,2$ if E is a regular h^2-parallelepiped.

Proof. For $j=0$ all three bounds follow immediately from (2.10). We have

$$\begin{aligned} DF_E = [&\mathbf{r}_{21}+(\mathbf{r}_{34}-\mathbf{r}_{21})\hat{y}+(\mathbf{r}_{65}-\mathbf{r}_{21})\hat{z}+((\mathbf{r}_{21}-\mathbf{r}_{34})-(\mathbf{r}_{65}-\mathbf{r}_{78}))\hat{y}\hat{z};\\ &\mathbf{r}_{41}+(\mathbf{r}_{34}-\mathbf{r}_{21})\hat{x}+(\mathbf{r}_{85}-\mathbf{r}_{41})\hat{z}+((\mathbf{r}_{21}-\mathbf{r}_{34})-(\mathbf{r}_{65}-\mathbf{r}_{78}))\hat{x}\hat{z};\\ &\mathbf{r}_{51}+(\mathbf{r}_{65}-\mathbf{r}_{21})\hat{x}+(\mathbf{r}_{85}-\mathbf{r}_{41})\hat{y}+((\mathbf{r}_{21}-\mathbf{r}_{34})-(\mathbf{r}_{65}-\mathbf{r}_{78}))\hat{x}\hat{y}], \end{aligned} \tag{3.2}$$

which implies $|DF|_{1,\infty,\hat{E}} \le Ch^2$ if E is an h^2-parallelepiped and $|DF|_{2,\infty,\hat{E}} \le Ch^3$ if E is a regular h^2-parallelepiped.

To show the second inequality in (3.1), we note that, for an h^2-parallelepiped, a simple calculation gives

$$J_E = a + b(\hat{x}+\hat{y}+\hat{z}) + c(\hat{x}\hat{y}+\hat{x}\hat{z}+\hat{y}\hat{z}) + d(\hat{x},\hat{y},\hat{z}), \tag{3.3}$$

where a, b, and c are constants,

$$|a| \le Ch^3,\ |b| \le Ch^4,\ |c| \le \begin{cases} Ch^4, & h^2-\text{parallelepiped} \\ Ch^5, & \text{regular } h^2-\text{parallelepiped}, \end{cases} \quad |d(\hat{x},\hat{y},\hat{z})| \le Ch^5.$$

Then

$$\left(\frac{1}{J_E}\right)_{\hat{x}} = -\frac{b+c(\hat{y}+\hat{z})+d_{\hat{x}}}{J_E^2},$$

with similar expressions for the other partial derivatives, which implies $|\frac{1}{J_E}|_{1,\infty,\hat{E}} \le Ch^{-2}$, using the bound on J_E in (2.10). Furthermore,

$$\left(\frac{1}{J_E}\right)_{\hat{x}\hat{y}} = -\frac{(c+d_{\hat{x}\hat{y}})J_E^2 - 2J_E(b+c(\hat{y}+\hat{z})+d_{\hat{x}})^2}{J_E^4},$$

with similar expressions for the other second derivatives, which implies $|\frac{1}{J_E}|_{2,\infty,\hat{E}} \le Ch^{-1}$ if E is a regular h^2-parallelepiped. We now have

$$\left|\frac{1}{J_E}DF_E\right|_{1,\infty,\hat{E}} \le \left|\frac{1}{J_E}\right|_{1,\infty,\hat{E}} |DF_E|_{0,\infty,\hat{E}} + \left|\frac{1}{J_E}\right|_{0,\infty,\hat{E}} |DF_E|_{1,\infty,\hat{E}} \le Ch^{-1},$$

if E is an h^2-parallelepiped and

$$\left|\frac{1}{J_E}DF_E\right|_{2,\infty,\hat{E}} \le \left|\frac{1}{J_E}\right|_{2,\infty,\hat{E}} |DF_E|_{0,\infty,\hat{E}} + \left|\frac{1}{J_E}\right|_{1,\infty,\hat{E}} |DF_E|_{1,\infty,\hat{E}} + \left|\frac{1}{J_E}\right|_{0,\infty,\hat{E}} |DF_E|_{2,\infty,\hat{E}} \le C,$$

if E is a regular h^2-parallelepiped.

To show the third inequality in (3.1), using the cofactor formula for the inverse of a matrix, we have that $J_E DF_E^{-1} = C_E^T$, where C_E is the cofactor matrix of DF_E. It is easy to see that each element of C_E is of the form

$$\alpha + \beta(\hat{x},\hat{y},\hat{z}) + \gamma(\hat{x},\hat{y},\hat{z}), \tag{3.4}$$

where α is a constant, β is a linear function, and, for an h^2-parallelepiped,

$$|\alpha| \le Ch^2, \quad |\beta| \le Ch^3, \text{ and } |\gamma| \le \begin{cases} Ch^3, & h^2-\text{parallelepiped}, \\ Ch^4, & \text{regular } h^2-\text{parallelepiped}. \end{cases}$$

This implies

$$|J_E DF_E^{-1}|_{1,\infty,\hat{E}} \le Ch^3$$

if E is an h^2-parallelepiped and

$$|J_E DF_E^{-1}|_{2,\infty,\hat{E}} \le Ch^4$$

if E is a regular h^2-parallelepiped. ∎

The above bounds allow us to control the norms of the reference element velocity vectors and permeability.

LEMMA 3.2. *For all $\mathbf{q} \in H^j(E)$, there exists a constant C independent of h such that the bound*

$$|\hat{\mathbf{q}}|_{j,\hat{E}} \le Ch^{j+1/2}\|\mathbf{q}\|_{j,E} \tag{3.5}$$

holds for $j = 0$ if E is a general hexahedron, for $j = 0, 1$ if E is an h^2-parallelepiped, and for $j = 0, 1, 2$ if E is a regular h^2-parallelepiped. Furthermore, on general hexahedra,

$$|\hat{\mathbf{q}}|_{1,\hat{E}} \le Ch^{1/2}\|\mathbf{q}\|_{1,E}. \tag{3.6}$$

Proof. The bound for $j = 0$ was shown in Lemma 2.5; see (2.43). We proceed with the cases $j = 1$ and 2. Let $\tilde{\mathbf{q}}(\hat{\mathbf{x}}) = \mathbf{q} \circ F_E(\hat{\mathbf{x}})$ and note that (2.12) implies that $\hat{\mathbf{q}}(\hat{\mathbf{x}}) = J_E DF_E^{-1}\tilde{\mathbf{q}}(\hat{\mathbf{x}})$. Using a change of variables, the chain rule, and (3.1), it is easy to see that

$$|\tilde{\mathbf{q}}|_{j,\hat{E}} \le Ch^{j-3/2}\|\mathbf{q}\|_{j,E}, \quad j = 0, 1, 2, \tag{3.7}$$

where the above equation holds for $j = 0, 1$ on general hexahedra and for $j = 2$ on h^2-parallelepipeds. We now have, for an h^2-parallelepiped,

$$\begin{aligned} |\hat{\mathbf{q}}|_{1,\hat{E}} &\le |J_E DF_E^{-1}|_{1,\infty,\hat{E}}|\tilde{\mathbf{q}}|_{0,\hat{E}} + |J_E DF_E^{-1}|_{0,\infty,\hat{E}}|\tilde{\mathbf{q}}|_{1,\hat{E}} \\ &\le C(h^3 h^{-3/2}|\mathbf{q}|_{0,E} + h^2 h^{-1/2}|\mathbf{q}|_{1,E}) \le Ch^{3/2}\|\mathbf{q}\|_{1,E}, \end{aligned} \tag{3.8}$$

where we have used (3.1) and (3.7) in the second inequality. Similarly, if E is a regular h^2-parallelepiped,

$$\begin{aligned}|\hat{\mathbf{q}}|_{2,\hat{E}} &\le |J_E DF_E^{-1}|_{2,\infty,\hat{E}} |\tilde{\mathbf{q}}|_{0,\hat{E}} + |J_E DF_E^{-1}|_{1,\infty,\hat{E}} |\tilde{\mathbf{q}}|_{1,\hat{E}} + |J_E DF_E^{-1}|_{0,\infty,\hat{E}} |\tilde{\mathbf{q}}|_{2,\hat{E}} \\ &\le C(h^4 h^{-3/2}|\mathbf{q}|_{0,E} + h^3 h^{-1/2}|\mathbf{q}|_{1,E} + h^2 h^{1/2}|\mathbf{q}|_{2,E}) \le Ch^{5/2}\|\mathbf{q}\|_{2,E}.\end{aligned}$$

The proof of (3.6) follows from (3.8), except that on general hexahedra we have only

$$|J_E DF_E^{-1}|_{1,\infty,\hat{E}} \le Ch^2.$$

The above bound follows from (3.4), noting that on general hexahedra $|\beta| + |\gamma| \le Ch^2$. ∎

LEMMA 3.3. *There exists a constant C independent of h such that the bound*

$$|\mathcal{K}^{-1}|_{j,\infty,\hat{E}} \le Ch^{j-1}\|K^{-1}\|_{j,\infty,E} \tag{3.9}$$

holds for $j = 0$ if E is a general hexahedron, for $j = 0, 1$ if E is an h^2-parallelepiped, and for $j = 0, 1, 2$ if E is a regular h^2-parallelepiped.

Proof. The bound for $j = 0$ was already shown above; see (2.32). Recall that

$$\mathcal{K}^{-1} = \frac{1}{J_E} DF_E^T \hat{K}^{-1} DF_E.$$

Using a change of variables, the chain rule, and (3.1), it is easy to see that

$$|\hat{K}^{-1}|_{j,\infty,\hat{E}} \le Ch^j |K^{-1}|_{j,\infty,E}, \tag{3.10}$$

where the above equation holds for $j = 0, 1$ on general hexahedra and for $j = 2$ on h^2-parallelepipeds. For an h^2-parallelepiped we have

$$\begin{aligned}&|\mathcal{K}^{-1}|_{1,\infty,\hat{E}} \\ &\quad\le \left|\frac{1}{J_E} DF_E^T\right|_{1,\infty,\hat{E}} |\hat{K}^{-1}|_{0,\infty,\hat{E}} |DF_E|_{0,\infty,\hat{E}} + \left|\frac{1}{J_E} DF_E^T\right|_{0,\infty,\hat{E}} |\hat{K}^{-1}|_{1,\infty,\hat{E}} |DF_E|_{0,\infty,\hat{E}} \\ &\qquad + \left|\frac{1}{J_E} DF_E^T\right|_{0,\infty,\hat{E}} |\hat{K}^{-1}|_{0,\infty,\hat{E}} |DF_E|_{1,\infty,\hat{E}} \\ &\quad\le C(h^{-1}h|K^{-1}|_{0,\infty,E} + h^{-2}h\,h|K^{-1}|_{1,\infty,E} + h^{-2}h^2|K^{-1}|_{0,\infty,E}) \le C\|K^{-1}\|_{1,\infty,E},\end{aligned}$$

where we have used (3.1) and (3.10) in the second inequality. Similarly, if E is a

regular h^2-parallelepiped,

$$
\begin{aligned}
&|\mathcal{K}^{-1}|_{2,\infty,\hat{E}} \\
&\quad\le \left(\left| \frac{1}{J_E} DF_E^T \right|_{2,\infty,\hat{E}} |DF_E|_{0,\infty,\hat{E}} + \left| \frac{1}{J_E} DF_E^T \right|_{1,\infty,\hat{E}} |DF_E|_{1,\infty,\hat{E}} \right. \\
&\qquad \left. + \left| \frac{1}{J_E} DF_E^T \right|_{0,\infty,\hat{E}} |DF_E|_{2,\infty,\hat{E}} \right) |\hat{K}^{-1}|_{0,\infty,\hat{E}} \\
&\qquad + \left(\left| \frac{1}{J_E} DF_E^T \right|_{1,\infty,\hat{E}} |DF_E|_{0,\infty,\hat{E}} + \left| \frac{1}{J_E} DF_E^T \right|_{0,\infty,\hat{E}} |DF_E|_{1,\infty,\hat{E}} \right) |\hat{K}^{-1}|_{1,\infty,\hat{E}} \\
&\qquad + \left| \frac{1}{J_E} DF_E^T \right|_{0,\infty,\hat{E}} |DF_E|_{0,\infty,\hat{E}} |\hat{K}^{-1}|_{2,\infty,\hat{E}} \\
&\quad\le C \left((h + h^{-1}h^2 + h^{-2}h^3)|K^{-1}|_{0,\infty,E} + (h^{-1}h + h^{-2}h^2)h|K^{-1}|_{1,\infty,E} \right. \\
&\qquad \left. + h^{-2}h\, h^2 |K^{-1}|_{2,\infty,E} \right) \\
&\quad\le Ch\|K^{-1}\|_{2,\infty,E}. \qquad \square
\end{aligned}
$$

We continue with establishing approximation properties for the mixed projection operators Π_* and Π_0 on hexahedra. We note that the original BDDF paper [13] and RT papers [44, 38, 37] did not consider hexahedral elements.

LEMMA 3.4. *There exists a constant C independent of h such that*

$$\|\mathbf{q} - \Pi_*\mathbf{q}\| + \|\mathbf{q} - \Pi_0\mathbf{q}\| \le Ch\|\mathbf{q}\|_1 \quad \textit{on } h^2 - \textit{parallelepipeds}, \tag{3.11}$$

$$\|\mathbf{q} - \Pi_*\mathbf{q}\| \le Ch^2\|\mathbf{q}\|_2 \quad \textit{on regular } h^2 - \textit{parallelepiped}, \tag{3.12}$$

$$|\nabla\cdot(\mathbf{q} - \Pi_*\mathbf{q})\| + \|\nabla\cdot(\mathbf{q} - \Pi_0\mathbf{q})\| \le Ch\|\nabla\cdot\mathbf{q}\|_1 \textit{ on } h^2 - \textit{parallelepipeds}. \tag{3.13}$$

Proof. We present the proof for Π_*. The arguments for Π_0 are similar. Using (2.43) and (3.5), we have for every element E

$$\|\mathbf{q} - \Pi_*\mathbf{q}\|_E \le Ch^{-1/2}\|\hat{\mathbf{q}} - \hat{\Pi}_*\hat{\mathbf{q}}\|_{\hat{E}} \le Ch^{-1/2}|\hat{\mathbf{q}}|_{j,\hat{E}} \le Ch^j\|\mathbf{q}\|_{j,E},$$

where $j = 1$ for an h^2-parallelepiped and $j = 2$ for a regular h^2-parallelepiped. In the second inequality above we used that $\hat{\Pi}_*$ preserves the constant and linear vectors and applied the Bramble–Hilbert lemma [20]. Summation over the elements completes the proof of (3.11) and (3.12).

For (3.13), using (2.14), we obtain

$$\int_E (\nabla\cdot(\mathbf{q} - \Pi_*\mathbf{q}))^2\,\mathrm{d}\mathbf{x} = \int_{\hat{E}} \frac{1}{J_E^2}(\hat{\nabla}\cdot(\hat{\mathbf{q}} - \hat{\Pi}_*\hat{\mathbf{q}}))^2 J_E\,\mathrm{d}\hat{\mathbf{x}} \le Ch^{-3}|\hat{\nabla}\cdot\hat{\mathbf{q}}|^2_{1,\hat{E}}, \tag{3.14}$$

where we have used (2.10), (2.28), and the Bramble–Hilbert lemma in the last inequality. Furthermore, using (3.3),

$$
\begin{aligned}
|\hat{\nabla}\cdot\hat{\mathbf{q}}|_{1,\hat{E}} &= |J_E\widehat{\nabla\cdot\mathbf{q}}|_{1,\hat{E}} \\
&\le C(\|J_E\|_{\infty,\hat{E}}|\widehat{\nabla\cdot\mathbf{q}}|_{1,\hat{E}} + |J_E|_{1,\infty,\hat{E}}\|\widehat{\nabla\cdot\mathbf{q}}\|_{\hat{E}}) \\
&\le C(h^3|\widehat{\nabla\cdot\mathbf{q}}|_{1,\hat{E}} + h^4\|\widehat{\nabla\cdot\mathbf{q}}\|_{\hat{E}}) \\
&\le C(h^3h\ h^{-3/2}|\nabla\cdot\mathbf{q}|_{1,E} + h^4h^{-3/2}\|\nabla\cdot\mathbf{q}\|_E) \\
&\le Ch^{5/2}\|\nabla\cdot\mathbf{q}\|_{1,E},
\end{aligned} \tag{3.15}
$$

where the next to last inequality follows from a change of variables back to E. A combination of (3.14) and (3.15) and a summation over the elements completes the proof of (3.13). ∎

Remark 3.1. The above result also applies to the BDDF projection operator Π from $\mathbf{V} \cap (H^1(\Omega))^3$ onto $\mathbf{V}_h$ on hexahedra, which extends the theory developed in [13] to such elements.

Let $\hat{Q}$ be the $L^2(\hat{E})$-orthogonal projection onto $\hat{W}(\hat{E})$, satisfying for any $\hat{\varphi} \in L^2(\hat{E})$,

$$(\hat{\varphi} - \hat{Q}\ \hat{\varphi}, \hat{w})_{\hat{E}} = 0 \quad \forall\, \hat{w} \in \hat{W}(\hat{E}).$$

Let $Q_h : L^2(\Omega) \to W_h$ be the projection operator, satisfying for any $\varphi \in L^2(\Omega)$,

$$Q_h\varphi = \hat{Q}\hat{\varphi} \circ F_E^{-1} \quad \text{on all } E.$$

It is easy to see that, due to (2.13),

$$(\varphi - Q_h\varphi, \nabla \cdot \mathbf{v}) = 0 \quad \forall\, \mathbf{v} \in \mathbf{V}_h^*. \tag{3.16}$$

Using a scaling argument similar to (3.14)–(3.15), we can show that on general hexahedra

$$\|\varphi - Q_h\varphi\| \le Ch|\varphi|_1. \tag{3.17}$$

For a scalar, vector, or tensor-valued function φ, let $\bar{\varphi}$ be its $L^2(E)$-projection onto the space of constant functions on E. It is known that [20]

$$\|\varphi - \bar{\varphi}\|_E \le Ch|\varphi|_{1,E}. \tag{3.18}$$

In the analysis we will make use of the following inverse inequality.

LEMMA 3.5. *For all elements E there exists a constant C independent of h such that*

$$\|\mathbf{q}\|_{j,E} \le Ch^{-1}\|\mathbf{q}\|_{j-1,E}, \quad j = 1, 2, \quad \forall\, \mathbf{q} \in \mathbf{V}_h^*(E). \tag{3.19}$$

Proof. The proof is based on a scaling argument and using the standard inverse inequality on $\hat{E}$. Let $\tilde{\mathbf{q}}(\hat{\mathbf{x}}) = \mathbf{q} \circ F_E(\hat{\mathbf{x}})$. For $j = 1$ we have, using a change of variables and (2.10),

$$\begin{aligned}|\mathbf{q}|_{1,E} &\le \|DF_E^{-1}\|_{0,\infty,E}\|J_E\|_{0,\infty,\hat{E}}^{1/2}|\tilde{\mathbf{q}}|_{1,\hat{E}} \le C\|DF_E^{-1}\|_{0,\infty,E}\|J_E\|_{0,\infty,\hat{E}}^{1/2}\|\tilde{\mathbf{q}}\|_{\hat{E}} \\ &\le C\|DF_E^{-1}\|_{0,\infty,E}\|J_E\|_{0,\infty,\hat{E}}^{1/2}\|J_{F_E{}^{-1}}\|_{0,\infty,E}^{1/2}\|\mathbf{q}\|_E \le Ch^{-1}\|\mathbf{q}\|_E.\end{aligned}$$

For $j = 2$, we note that [20, Chapter 4.3]

$$|DF_E^{-1}|_{1,\infty,E} \le |DF_E|_{1,\infty,\hat{E}}\|DF_E^{-1}\|_{0,\infty,E}^3 \le Ch^{-2},$$

using (2.10) and (3.1) on general hexahedra in the last inequality. Therefore, using a change of variables,

$$\begin{aligned}|\mathbf{q}|_{2,E} &\le (\|DF_E^{-1}\|_{0,\infty,E}^2|\tilde{\mathbf{q}}|_{2,\hat{E}} + |DF_E^{-1}|_{1,\infty,E}|\tilde{\mathbf{q}}|_{1,\hat{E}})\|J_E\|_{0,\infty,\hat{E}}^{1/2} \\ &\le Ch^{-2}\|J_E\|_{0,\infty,\hat{E}}^{1/2}(|\tilde{\mathbf{q}}|_{1,\hat{E}} + |\tilde{\mathbf{q}}|_{2,\hat{E}}) \\ &\le Ch^{-2}\|J_E\|_{0,\infty,\hat{E}}^{1/2}|\tilde{\mathbf{q}}|_{1,\hat{E}} \\ &\le Ch^{-2}\|J_E\|_{0,\infty,\hat{E}}^{1/2}\|DF_E\|_{0,\infty,\hat{E}}\|J_{F_E{}^{-1}}\|_{0,\infty,E}^{1/2}|\mathbf{q}|_{1,E} \\ &\le Ch^{-1}|\mathbf{q}|_{1,E}. \quad ∎\end{aligned}$$

We next establish some continuity bounds for Π_* and Π_0.

LEMMA 3.6. *There exists a constant C independent of h such that*

$$\|\Pi_*\mathbf{q}\|_{j,E} \le C\|\mathbf{q}\|_{j,E} \quad \forall \mathbf{q} \in (H^j(E))^3, \quad j = 1, 2, \tag{3.20}$$

where the above holds for $j = 1$ on h^2-parallelepipeds and $j = 1, 2$ on regular h^2-parallelepipeds. Furthermore, on h^2-parallelepipeds,

$$\|\Pi_0\mathbf{q}\|_{1,E} \le C\|\mathbf{q}\|_{1,E} \quad \forall \mathbf{q} \in (H^1(E))^3, \tag{3.21}$$

and on general hexahedra,

$$\|\Pi_*\mathbf{q}\|_{\mathrm{div},E} + \|\Pi_0\mathbf{q}\|_{\mathrm{div},E} \le C\|\mathbf{q}\|_{1,E} \quad \forall \mathbf{q} \in (H^1(E))^3. \tag{3.22}$$

Proof. Using (3.19) we have

$$\begin{aligned} |\Pi_*\mathbf{q}|_{1,E} &= |\Pi_*\mathbf{q} - \bar{\mathbf{q}}|_{1,E} \le Ch^{-1}\|\Pi_*\mathbf{q} - \bar{\mathbf{q}}\|_E \\ &\le Ch^{-1}(\|\Pi_*\mathbf{q} - \mathbf{q}\|_E + \|\mathbf{q} - \bar{\mathbf{q}}\|_E) \le C\|\mathbf{q}\|_{1,E}, \end{aligned}$$

using (3.11) and (3.18) for the last inequality.

Similarly, taking $\mathbf{q}_1$ to be the $L^2(E)$-projection of $\mathbf{q}$ onto the space of linear vectors on E, we obtain

$$\begin{aligned} |\Pi_*\mathbf{q}|_{2,E} &= |\Pi_*\mathbf{q} - \mathbf{q}_1|_{2,E} \le Ch^{-2}\|\Pi_*\mathbf{q} - \mathbf{q}_1\|_E \\ &\le Ch^{-2}(\|\Pi_*\mathbf{q} - \mathbf{q}\|_E + \|\mathbf{q} - \mathbf{q}_1\|_E) \le C\|\mathbf{q}\|_{2,E}, \end{aligned}$$

using (3.12) and the approximation property $\|\mathbf{q} - \mathbf{q}_1\|_E \le Ch^2|\mathbf{q}|_{2,E}$ [20] for the last inequality.

The bound $\|\Pi_*\mathbf{q}\|_E \le C\|\mathbf{q}\|_{1,E}$ for an h^2-parallelepiped follows from the approximation property (3.11). This completes the proof of (3.20). The proof of (3.21) is similar.

We continue with the proof of (3.22). For a general hexahedron E, using (2.14) and (2.10), we obtain, similarly to (3.14)–(3.15),

$$\begin{aligned} \|\nabla \cdot \Pi_*\mathbf{q}\|_E &\le Ch_E^{-3/2}\|\hat{\nabla} \cdot \hat{\Pi}_*\hat{\mathbf{q}}\|_{\hat{E}} \le Ch_E^{-3/2}\|\hat{\nabla} \cdot \hat{\mathbf{q}}\|_{\hat{E}} \\ &= Ch_E^{-3/2}\|J_E\widehat{\nabla \cdot \mathbf{q}}\|_{\hat{E}} \le C\|\nabla \cdot \mathbf{q}\|_E, \end{aligned} \tag{3.23}$$

where we have also used that $\hat{\nabla} \cdot \hat{\Pi}_*\hat{\mathbf{q}}$ is the $L^2(\hat{E})$-projection of $\hat{\nabla} \cdot \hat{\mathbf{q}}$ (see (2.28)) for the second inequality. Next, using (2.43), the Bramble–Hilbert lemma, and (3.6),

$$\begin{aligned} \|\Pi_*\mathbf{q}\|_E &\le Ch^{-1/2}\|\hat{\Pi}_*\hat{\mathbf{q}}\|_{\hat{E}} \le Ch^{-1/2}(\|\hat{\Pi}_*\hat{\mathbf{q}} - \hat{\mathbf{q}}\|_{\hat{E}} + \|\hat{\mathbf{q}}\|_{\hat{E}}) \\ &\le Ch^{-1/2}(|\hat{\mathbf{q}}|_{1,\hat{E}} + \|\hat{\mathbf{q}}\|_{\hat{E}}) \le C\|\mathbf{q}\|_{1,E}. \end{aligned} \tag{3.24}$$

A combination of (3.23) and (3.23) implies that

$$\|\Pi_*\mathbf{q}\|_{\mathrm{div},E} \le C\|\mathbf{q}\|_{1,E}.$$

The argument for $\|\Pi_0\mathbf{q}\|_{\mathrm{div},E}$ is the same. ∎

For the permeability tensor K we will use the following notation. Let $W^{k,p}_{\mathcal{T}_h}$ consist of functions φ such that $\varphi|_E \in W^{k,p}(E)$ $\forall E \in \mathcal{T}_h$, and $\|\varphi\|_{k,p,E}$ is uniformly bounded, independently of h. Let $|||\varphi|||_{k,p} = \max_{E\in\mathcal{T}_h} \|\varphi\|_{k,p,E}$.

We conclude the subsection with an approximation result needed in the analysis.

LEMMA 3.7. *On h^2-parallelepipeds, if $K^{-1} \in W^{1,\infty}_{\mathcal{T}_h}$, then there exists a constant C independent of h such that for all $\mathbf{v} \in \mathbf{V}_h$*

$$|(K^{-1}\Pi_* \mathbf{u}, \mathbf{v} - \Pi_0 \mathbf{v})_Q| \le Ch\|\mathbf{u}\|_1 \|\mathbf{v}\|. \tag{3.25}$$

Proof. On any element E we have

$$\begin{aligned}(K^{-1}\Pi_* \mathbf{u}, \mathbf{v} - \Pi_0 \mathbf{v})_{Q,E} &= (\mathcal{K}^{-1}\hat{\Pi}_* \hat{\mathbf{u}}, \hat{\mathbf{v}} - \hat{\Pi}_0 \hat{\mathbf{v}})_{\hat{Q},\hat{E}} \\ &= ((\mathcal{K}^{-1} - \overline{\mathcal{K}^{-1}})\hat{\Pi}_* \hat{\mathbf{u}}, \hat{\mathbf{v}} - \hat{\Pi}_0 \hat{\mathbf{v}})_{\hat{Q},\hat{E}} \\ &\quad + (\overline{\mathcal{K}^{-1}}\hat{\Pi}_* \hat{\mathbf{u}}, \hat{\mathbf{v}} - \hat{\Pi}_0 \hat{\mathbf{v}})_{\hat{Q},\hat{E}}.\end{aligned} \tag{3.26}$$

Using the Bramble–Hilbert lemma and (2.45), we have for the first term on the right above

$$\begin{aligned}|((\mathcal{K}^{-1} - \overline{\mathcal{K}^{-1}})\hat{\Pi}_* \hat{\mathbf{u}}, \hat{\mathbf{v}} - \hat{\Pi}_0 \hat{\mathbf{v}})_{\hat{Q},\hat{E}}| &\le C|\mathcal{K}^{-1}|_{1,\infty,\hat{E}} \|\hat{\Pi}_* \hat{\mathbf{u}}\|_{\hat{E}} \|\hat{\mathbf{v}}\|_{\hat{E}} \\ &\le C\|K^{-1}\|_{1,\infty,E} h^{1/2} \|\mathbf{u}\|_{1,E} h^{1/2} \|\mathbf{v}\|_E,\end{aligned} \tag{3.27}$$

where we have used (3.9), (3.5), and (3.20) for the last inequality. Using (2.39), we have for the last term in (3.26)

$$\begin{aligned}|(\overline{\mathcal{K}^{-1}}\hat{\Pi}_* \hat{\mathbf{u}}, \hat{\mathbf{v}} - \hat{\Pi}_0 \hat{\mathbf{v}})_{\hat{Q},\hat{E}}| &= |(\overline{\mathcal{K}^{-1}}(\hat{\Pi}_* \hat{\mathbf{u}} - \overline{\hat{\Pi}_* \hat{\mathbf{u}}}), \hat{\mathbf{v}} - \hat{\Pi}_0 \hat{\mathbf{v}})_{\hat{Q},\hat{E}}| \\ &\le C\|\mathcal{K}^{-1}\|_{0,\infty,\hat{E}} |\hat{\Pi}_* \hat{\mathbf{u}}|_{1,\hat{E}} \|\hat{\mathbf{v}}\|_{\hat{E}} \\ &\le Ch^{-1}\|K^{-1}\|_{0,\infty,E} h^{3/2} \|\mathbf{u}\|_{1,E} h^{1/2} \|\mathbf{v}\|_E,\end{aligned} \tag{3.28}$$

where we have also used the Bramble–Hilbert lemma, (3.9), (3.5), and (3.20). The proof is completed by combining (3.26)–(3.28). ∎

3.2. First-order convergence for the velocity.

THEOREM 3.1. *On h^2-parallelepipeds, if $K^{-1} \in W^{1,\infty}_{\mathcal{T}_h}$, then, for the velocity $\mathbf{u}_h$ of the MFMFE method* (2.41)–(2.42)*, there exists a constant C independent of h such that*

$$\|\mathbf{u} - \mathbf{u}_h\| \le Ch\|\mathbf{u}\|_1, \tag{3.29}$$

$$\|\nabla \cdot (\mathbf{u} - \mathbf{u}_h)\| \le Ch\|\nabla \cdot \mathbf{u}\|_1. \tag{3.30}$$

Proof. The following error equations are obtained by subtracting the numerical scheme (2.41)–(2.42) from the variational formulation (2.6)–(2.7):

$$\begin{aligned}(K^{-1}(\Pi_* \mathbf{u} - \mathbf{u}_h), \mathbf{v})_Q &= (Q_h p - p_h, \nabla \cdot \mathbf{v}) - \langle g, (\mathbf{v} - \Pi_0 \mathbf{v}) \cdot \mathbf{n} \rangle_{\Gamma_D} \\ &\quad - (K^{-1}\mathbf{u}, \mathbf{v}) + (K^{-1}\Pi_* \mathbf{u}, \mathbf{v})_Q, \quad \mathbf{v} \in \mathbf{V}_h^*,\end{aligned} \tag{3.31}$$

$$(\nabla \cdot (\Pi_* \mathbf{u} - \mathbf{u}_h), w) = 0, \quad w \in W_h, \tag{3.32}$$

where we have used the orthogonality property of $\mathcal{P}_0$ (2.40) to rewrite the error term on Γ_D. For the last two terms in (3.31) we write

$$\begin{aligned}&-(K^{-1}\mathbf{u}, \mathbf{v}) + (K^{-1}\Pi_* \mathbf{u}, \mathbf{v})_Q = -(K^{-1}\mathbf{u}, \mathbf{v} - \Pi_0 \mathbf{v}) - (K^{-1}(\mathbf{u} - \Pi_* \mathbf{u}), \Pi_0 \mathbf{v}) \\ &\quad - (K^{-1}\Pi_* \mathbf{u}, \Pi_0 \mathbf{v}) + (K^{-1}\Pi_* \mathbf{u}, \Pi_0 \mathbf{v})_Q + (K^{-1}\Pi_* \mathbf{u}, \mathbf{v} - \Pi_0 \mathbf{v})_Q.\end{aligned} \tag{3.33}$$

For the first term on the right above we have

$$-(K^{-1}\mathbf{u}, \mathbf{v} - \Pi_0\mathbf{v}) - \langle g, (\mathbf{v} - \Pi_0\mathbf{v}) \cdot \mathbf{n}\rangle_{\Gamma_D} = 0, \tag{3.34}$$

which follows by taking $\mathbf{v} - \Pi_0\mathbf{v}$ as a test function in the variational formulation (2.6) and using (2.22). Using (3.11) and (2.23), the second term on the right in (3.33) can be bounded as

$$|(K^{-1}(\mathbf{u} - \Pi_*\mathbf{u}), \Pi_0\mathbf{v})| \le Ch\|K^{-1}\|_{0,\infty}\|\mathbf{u}\|_1\|\mathbf{v}\|. \tag{3.35}$$

The third and forth term on the right in (3.33) represent the quadrature error, which can be bounded by Lemma 3.8 as

$$|\sigma(K^{-1}\Pi_*\mathbf{u}, \Pi_0\mathbf{v})| \le Ch|||K^{-1}|||_{1,\infty}\|\mathbf{u}\|_1\|\mathbf{v}\|, \tag{3.36}$$

using also (3.20) and (2.23). The last term on the right in (3.33) is bounded in Lemma 3.7.

We next note that

$$\nabla \cdot (\Pi_*\mathbf{u} - \mathbf{u}_h) = 0, \tag{3.37}$$

since, due to (2.14), we can choose $w = J_E\nabla \cdot (\Pi_*\mathbf{u} - \mathbf{u}_h) \in W_h$ on any element E in (3.32) and J_E is uniformly positive. Taking $\mathbf{v} = \Pi_*\mathbf{u} - \mathbf{u}_h$ in the error equation (3.31) above and combining (3.33)–(3.36) with (2.45) and (3.25), we obtain

$$\|\Pi_*\mathbf{u} - \mathbf{u}_h\| \le Ch|||K^{-1}|||_{1,\infty}\|\mathbf{u}\|_1. \tag{3.38}$$

The assertion of the theorem follows from (3.38), (3.37), (3.11), and (3.13). ∎

The following lemma provides a bound on the quadrature error.

LEMMA 3.8. *On h^2-parallelepipeds, if $K^{-1} \in W^{1,\infty}_{\mathcal{T}_h}$, then there exists a constant C independent of h such that for all $\mathbf{q} \in \mathbf{V}^*_h$ and for all $\mathbf{v} \in \mathbf{V}^0_h$*

$$|\sigma(K^{-1}\mathbf{q}, \mathbf{v})| \le C \sum_{E\in\mathcal{T}_h} h\|K^{-1}\|_{1,\infty,E}\|\mathbf{q}\|_{1,E}\|\mathbf{v}\|_E. \tag{3.39}$$

Proof. On any element E we have

$$\sigma_E(K^{-1}\mathbf{q}, \mathbf{v}) = \hat{\sigma}_{\hat{E}}(\mathcal{K}^{-1}\hat{\mathbf{q}}, \hat{\mathbf{v}}) = \hat{\sigma}_{\hat{E}}((\mathcal{K}^{-1} - \overline{\mathcal{K}^{-1}})\hat{\mathbf{q}}, \hat{\mathbf{v}}) + \hat{\sigma}_{\hat{E}}(\overline{\mathcal{K}^{-1}}\hat{\mathbf{q}}, \hat{\mathbf{v}}). \tag{3.40}$$

Using the Bramble–Hilbert lemma, the first term on the right above can be bounded as

$$|\hat{\sigma}_{\hat{E}}((\mathcal{K}^{-1} - \overline{\mathcal{K}^{-1}})\hat{\mathbf{q}}, \hat{\mathbf{v}})| \le C|\mathcal{K}^{-1}|_{1,\infty,\hat{E}}\|\hat{\mathbf{q}}\|_{\hat{E}}\|\hat{\mathbf{v}}\|_{\hat{E}} \le C\|K^{-1}\|_{1,\infty,E}h^{1/2}\|\mathbf{q}\|_E h^{1/2}\|\mathbf{v}\|_E, \tag{3.41}$$

where we used (3.9) and (3.5) for the last inequality. For the last term in (3.40) we have that $\hat{\sigma}_{\hat{E}}(\overline{\mathcal{K}^{-1}}\hat{\mathbf{q}}_0, \hat{\mathbf{v}}) = 0$ for any constant vector $\hat{\mathbf{q}}_0$, since the trapezoidal quadrature rule $(\cdot,\cdot)_{\hat{Q},\hat{E}}$ is exact for linear functions. Hence the Bramble–Hilbert lemma implies

$$|\hat{\sigma}_{\hat{E}}(\overline{\mathcal{K}^{-1}}\hat{\mathbf{q}}, \hat{\mathbf{v}})| \le C\|\mathcal{K}^{-1}\|_{0,\infty,\hat{E}}|\hat{\mathbf{q}}|_{1,\hat{E}}\|\hat{\mathbf{v}}\|_{\hat{E}}.$$

Using (3.9) and (3.5), we obtain

$$|\hat{\sigma}_{\hat{E}}(\overline{\mathcal{K}^{-1}}\hat{\mathbf{q}}, \hat{\mathbf{v}})| \le Ch^{-1}\|K^{-1}\|_{0,\infty,E}h^{3/2}\|\mathbf{q}\|_{1,E}h^{1/2}\|\mathbf{v}\|_E. \tag{3.42}$$

The above bound, together with (3.40)–(3.41), implies

$$|\sigma_E(K^{-1}\mathbf{q}, \mathbf{v})| \le Ch\|K^{-1}\|_{1,\infty,E}\|\mathbf{q}\|_{1,E}\|\mathbf{v}\|_E.$$

The proof is completed by summing over all elements E. ∎

4. Error estimates for the pressure. We first employ a standard inf-sup argument to prove optimal convergence for the pressure on h^2-parallelepipeds. Then, using a duality argument, we establish superconvergence for the pressure at the element centers of mass on regular h^2-parallelepipeds.

4.1. First-order convergence for the pressure.

THEOREM 4.1. *On h^2-parallelepipeds, if $K^{-1} \in W^{1,\infty}_{\mathcal{T}_h}$, then, for the pressure p_h of the MFMFE method* (2.41)–(2.42)*, there exists a constant C independent of h such that*

$$\|p - p_h\| \le Ch(\|\mathbf{u}\|_1 + \|p\|_1).$$

Proof. We first note that the RT_0 spaces $\mathbf{V}_h^0 \times W_h^0$ on hexahedra satisfy the inf-sup condition

$$\inf_{0\neq w\in W_h^0} \sup_{0\neq \mathbf{v}\in \mathbf{V}_h^0} \frac{(\nabla\cdot\mathbf{v}, w)}{\|\mathbf{v}\|_{\mathrm{div}}\|w\|} \ge \beta, \tag{4.1}$$

where β is a positive constant independent of h. The proof of (4.1) uses a standard approach [15, 26]. In particular, for a given $w \in W_h^0$ we consider the auxiliary problem (2.46) with p_h replaced by w and recall that there exists a solution $\boldsymbol{\psi} \in H^1(\Omega)$ that satisfies the regularity bound (2.47).

Taking $\mathbf{v} = \Pi_0\boldsymbol{\psi} \in \mathbf{V}_h^0$ and using the properties of Π_0 (2.21) and (3.22) as well as (2.47), we have

$$\frac{(\nabla\cdot\mathbf{v}, w)}{\|\mathbf{v}\|_{\mathrm{div}}\|w\|} = \frac{(\nabla\cdot\boldsymbol{\psi}, w)}{\|\Pi_0\boldsymbol{\psi}\|_{\mathrm{div}}\|w\|} \ge \frac{1}{C}\frac{\|w\|^2}{\|\boldsymbol{\psi}\|_1\|w\|} \ge \frac{1}{C} \equiv \beta.$$

Using (4.1) and (3.31), we obtain

$$\begin{aligned}
&\|\mathcal{Q}_h p - p_h\| \\
&\quad\le \frac{1}{\beta}\sup_{0\neq\mathbf{v}\in\mathbf{V}_h^0} \frac{(\nabla\cdot\mathbf{v}, \mathcal{Q}_h p - p_h)}{\|\mathbf{v}\|_{\mathrm{div}}} \\
&\quad= \frac{1}{\beta}\sup_{0\neq\mathbf{v}\in\mathbf{V}_h^0} \frac{(K^{-1}(\Pi_*\mathbf{u} - \mathbf{u}_h), \mathbf{v})_Q - (K^{-1}(\Pi_*\mathbf{u} - \mathbf{u}), \mathbf{v}) + \sigma(K^{-1}\Pi_*\mathbf{u}, \mathbf{v})}{\|\mathbf{v}\|_{\mathrm{div}}} \\
&\quad\le \frac{C}{\beta} h \|\!| K^{-1} |\!\|_{1,\infty} \|\mathbf{u}\|_1,
\end{aligned}$$

where we have used the Cauchy–Schwarz inequality, (3.38), (3.11), (3.39), and (3.20) in the last inequality. The assertion of the theorem follows from an application of the triangle inequality and (3.17). ∎

4.2. Second-order convergence for the pressure. In this section we establish second-order convergence for the pressure on regular h^2-parallelepipeds. The following bound on the quadrature error will be used in the superconvergence analysis.

LEMMA 4.1. *On regular h^2-parallelepipeds, if $K^{-1} \in W^{2,\infty}_{\mathcal{T}_h}$, then for all $\mathbf{q} \in \mathbf{V}_h^*$ and $\mathbf{v} \in \mathbf{V}_h^0$, there exists a positive constant C independent of h such that*

$$|\sigma(K^{-1}\mathbf{q}, \mathbf{v})| \le C \sum_{E\in\mathcal{T}_h} h^2 \|K^{-1}\|_{2,\infty,E}\|\mathbf{q}\|_{2,E}\|\mathbf{v}\|_{1,E}. \tag{4.2}$$

Proof. For any element E we have $\sigma_E(K^{-1}\mathbf{q},\mathbf{v}) = \hat{\sigma}_{\hat{E}}(\mathcal{K}^{-1}\hat{\mathbf{q}},\hat{\mathbf{v}})$. Since the trapezoidal quadrature rule is exact for linear functions, the Peano Kernel theorem [43] implies

(4.3)
$$\begin{aligned}\hat{\sigma}_{\hat{E}}(\mathcal{K}^{-1}\hat{\mathbf{q}},\hat{\mathbf{v}}) = \int_{\hat{E}} \Big(&\varphi(\hat{x})\frac{\partial^2}{\partial\hat{x}^2}(\mathcal{K}^{-1}\hat{\mathbf{q}}\cdot\hat{\mathbf{v}})(\hat{x},0,0) + \varphi(\hat{y})\frac{\partial^2}{\partial\hat{y}^2}(\mathcal{K}^{-1}\hat{\mathbf{q}}\cdot\hat{\mathbf{v}})(0,\hat{y},0)\\ &+ \varphi(\hat{z})\frac{\partial^2}{\partial\hat{z}^2}(\mathcal{K}^{-1}\hat{\mathbf{q}}\cdot\hat{\mathbf{v}})(0,0,\hat{z}) + \psi(\hat{x},\hat{y})\frac{\partial^2}{\partial\hat{x}\partial\hat{y}}(\mathcal{K}^{-1}\hat{\mathbf{q}}\cdot\hat{\mathbf{v}})(\hat{x},\hat{y},0)\\ &+ \psi(\hat{x},\hat{z})\frac{\partial^2}{\partial\hat{x}\partial\hat{z}}(\mathcal{K}^{-1}\hat{\mathbf{q}}\cdot\hat{\mathbf{v}})(\hat{x},0,\hat{z})\\ &+ \psi(\hat{y},\hat{z})\frac{\partial^2}{\partial\hat{y}\partial\hat{z}}(\mathcal{K}^{-1}\hat{\mathbf{q}}\cdot\hat{\mathbf{v}})(0,\hat{y},\hat{z})\Big)\,d\hat{x}\,d\hat{y}\,d\hat{z},\end{aligned}$$

where φ and ψ are bounded functions. Therefore, using that $\hat{\mathbf{v}}$ is linear,

$$\begin{aligned}|\hat{\sigma}_{\hat{E}}(\mathcal{K}^{-1}\hat{\mathbf{q}},\hat{\mathbf{v}})| \le& C((|\mathcal{K}^{-1}|_{1,\infty,\hat{E}}\|\hat{\mathbf{q}}\|_{\hat{E}} + \|\mathcal{K}^{-1}\|_{0,\infty,\hat{E}}|\hat{\mathbf{q}}|_{1,\hat{E}})|\hat{\mathbf{v}}|_{1,\hat{E}}\\ &+ (|\mathcal{K}^{-1}|_{2,\infty,\hat{E}}\|\hat{\mathbf{q}}\|_{\hat{E}} + |\mathcal{K}^{-1}|_{1,\infty,\hat{E}}|\hat{\mathbf{q}}|_{1,\hat{E}} + \|\mathcal{K}^{-1}\|_{0,\infty,\hat{E}}|\hat{\mathbf{q}}|_{2,\hat{E}})\|\hat{\mathbf{v}}\|_{\hat{E}}).\end{aligned}$$

Using (3.9) and (3.5), we obtain

$$|\sigma_E(K^{-1}\mathbf{q},\mathbf{v})| \le Ch^2\|K^{-1}\|_{2,\infty,E}\|\mathbf{q}\|_{2,E}\|\mathbf{v}\|_{1,E}.$$

Summing over all elements completes the proof. ∎

The following result establishes superconvergence of the pressure at the cell centers. The proof is similar to the argument of Theorem 4.3 in [48], but it uses bounds for regular h^2-parallelepipeds established in the previous sections.

THEOREM 4.2. *Assume that the partition $\mathcal{T}_h$ consists of regular h^2-parallelepipeds, $K \in W^{1,\infty}_{\mathcal{T}_h}$, $K^{-1} \in W^{2,\infty}_{\mathcal{T}_h}$, and the elliptic regularity* (4.5) *below holds. Then, for the pressure p_h of the MFMFE method* (2.41)–(2.42)*, there exists a constant C independent of h such that*

$$\|\mathcal{Q}_h p - p_h\| \le Ch^2\|\mathbf{u}\|_2. \tag{4.4}$$

Proof. The proof is based on a duality argument. Let ϕ be the solution to

$$\begin{aligned} -\nabla\cdot K\nabla\phi &= -(\mathcal{Q}_h p - p_h) && \text{in } \Omega,\\ \phi &= 0 && \text{on } \Gamma_D,\\ -K\nabla\phi\cdot\mathbf{n} &= 0 && \text{on } \Gamma_N.\end{aligned}$$

We assume that this problem is H^2-elliptic regular:

$$\|\phi\|_2 \le C\|\mathcal{Q}_h p - p_h\|. \tag{4.5}$$

Sufficient conditions for (4.5) can be found in [27, 34]. For example, (4.5) holds if the components of $K \in C^{0,1}(\overline{\Omega})$, $\partial\Omega$ are smooth enough and either Γ_D or Γ_N is empty.

It is convenient to rewrite the error equation (3.31) in the form

$$\begin{aligned}(K^{-1}(\Pi_*\mathbf{u} - \mathbf{u}_h),\mathbf{v})_Q =& (Q_h p - p_h, \nabla\cdot\mathbf{v}) + (K^{-1}(\Pi_*\mathbf{u} - \mathbf{u}),\mathbf{v})\\ &- \sigma(K^{-1}\Pi_*\mathbf{u},\mathbf{v}) - \langle g,(\mathbf{v} - \Pi_0\mathbf{v})\cdot\mathbf{n}\rangle_{\Gamma_D}.\end{aligned} \tag{4.6}$$

Take $\mathbf{v} = \Pi_0 K \nabla \phi \in \mathbf{V}_h$ in (4.6) to get

$$\begin{aligned}\|\mathcal{Q}_h p - p_h\|^2 &= (\mathcal{Q}_h p - p_h, \nabla \cdot \Pi_0 K \nabla \phi) \\ &= (K^{-1}(\Pi_* \mathbf{u} - \mathbf{u}_h), \Pi_0 K \nabla \phi)_Q - (K^{-1}(\Pi_* \mathbf{u} - \mathbf{u}), \Pi_0 K \nabla \phi) \\ &\quad + \sigma(K^{-1}\Pi_* \mathbf{u}, \Pi_0 K \nabla \phi). \end{aligned} \tag{4.7}$$

For the second term on the right above, (3.12) and (3.21) imply that

$$|(K^{-1}(\Pi_* \mathbf{u} - \mathbf{u}), \Pi_0 K \nabla \phi)| \le C h^2 \|K^{-1}\|_{0,\infty} |\!|\!| K |\!|\!|_{1,\infty} \|\mathbf{u}\|_2 \|\phi\|_2. \tag{4.8}$$

Using (4.2), (3.20), and (3.21), the last term on the right in (4.7) can be bounded as

$$\sigma(K^{-1}\Pi_* \mathbf{u}, \Pi_0 K \nabla \phi) \le C h^2 |\!|\!| K^{-1} |\!|\!|_{2,\infty} |\!|\!| K |\!|\!|_{1,\infty} \|\mathbf{u}\|_2 \|\phi\|_2. \tag{4.9}$$

The first term on the right in (4.7) can be manipulated as follows:

$$\begin{aligned}&(K^{-1}(\Pi_* \mathbf{u} - \mathbf{u}_h), \Pi_0 K \nabla \phi)_{Q,E} \\ &\quad = ((K^{-1} - \overline{K}^{-1})(\Pi_* \mathbf{u} - \mathbf{u}_h), \Pi_0 K \nabla \phi)_{Q,E} + (\overline{K}^{-1}(\Pi_* \mathbf{u} - \mathbf{u}_h), \Pi_0 (K - \overline{K}) \nabla \phi)_{Q,E} \\ &\qquad + (\overline{K}^{-1}(\Pi_* \mathbf{u} - \mathbf{u}_h), \Pi_0 \overline{K}(\nabla \phi - \nabla \phi_1))_{Q,E} \\ &\qquad + (\overline{K}^{-1}(\Pi_* \mathbf{u} - \mathbf{u}_h), \Pi_0 \overline{K} \nabla \phi_1 - \overline{K} \nabla \phi_1)_{Q,E} \\ &\qquad + (\Pi_* \mathbf{u} - \mathbf{u}_h), \nabla \phi_1)_{Q,E} \end{aligned} \tag{4.10}$$

where ϕ_1 is a linear approximation to ϕ such that (see [12])

$$\|\phi - \phi_1\|_E \le C h^2 \|\phi\|_{2,E}, \quad \|\phi - \phi_1\|_{1,E} \le C h \|\phi\|_{2,E}. \tag{4.11}$$

Since $K^{-1} - \overline{K}^{-1} = \overline{K}^{-1}(\overline{K} - K)K^{-1}$, using (2.5) we have that for each $\mathbf{x} \in \Omega$

$$|(K^{-1} - \overline{K}^{-1})\xi \cdot \eta| \le \frac{1}{k_0^2} \|K - \overline{K}\|_{\mathbb{R}^{3\times 3}} \|\xi\|_{\mathbb{R}^3} \|\eta\|_{\mathbb{R}^3} \quad \forall \xi, \eta \in \mathbb{R}^3,$$

where $\|\cdot\|_{\mathbb{R}^{3\times 3}}$ is the matrix norm induced by the Euclidean vector norm $\|\cdot\|_{\mathbb{R}^3}$. Therefore, using (3.18) and (3.21), the first term on the right in (4.10) can be bounded as

$$|((K^{-1} - \overline{K}^{-1})(\Pi_* \mathbf{u} - \mathbf{u}_h), \Pi_0 K \nabla \phi)_{Q,E}| \le \frac{C}{k_0^2} h \|K\|_{1,\infty,E}^2 \|\Pi_* \mathbf{u} - \mathbf{u}_h\|_E \|\phi\|_{2,E}. \tag{4.12}$$

To bound the second and third terms on the right in (4.10), first note that for any $\boldsymbol{\psi} \in (H^1(E))^3$

$$\|\Pi_0 \boldsymbol{\psi}\|_E \le \|\Pi_0 \boldsymbol{\psi} - \boldsymbol{\psi}\|_E + \|\boldsymbol{\psi}\|_E \le C(h \|\boldsymbol{\psi}\|_{1,E} + \|\boldsymbol{\psi}\|_E).$$

Then we have

$$|(\overline{K}^{-1}(\Pi_* \mathbf{u} - \mathbf{u}_h), \Pi_0 (K - \overline{K}) \nabla \phi)_{Q,E}| \le \frac{C}{k_0} h \|K\|_{1,\infty,E} \|\Pi_* \mathbf{u} - \mathbf{u}_h\|_E \|\phi\|_{2,E} \tag{4.13}$$

and

$$|(\overline{K}^{-1}(\Pi_* \mathbf{u} - \mathbf{u}_h), \Pi_0 \overline{K}(\nabla \phi - \nabla \phi_1))_{Q,E}| \le \frac{C}{k_0} h \|K\|_{0,\infty,E} \|\Pi_* \mathbf{u} - \mathbf{u}_h\|_E \|\phi\|_{2,E}, \tag{4.14}$$

where we have also used (4.11) in the last inequality. The fourth term on the right in (4.10) can be bounded using (3.11):

$$(\overline{K}^{-1}(\Pi_*\mathbf{u}-\mathbf{u}_h),\Pi_0\overline{K}\nabla\phi_1-\overline{K}\nabla\phi_1)_{Q,E}\le\frac{C}{k_0}h\|K\|_{0,\infty,E}\|\Pi_*\mathbf{u}-\mathbf{u}_h\|_E\|\phi\|_{2,E},$$

For the last term in (4.10) we have

$$(\Pi_*\mathbf{u}-\mathbf{u}_h,\nabla\phi_1)_{Q,E}=(\hat{\Pi}_*\hat{\mathbf{u}}-\hat{\mathbf{u}}_h,\hat{\nabla}\hat{\phi}_1)_{\hat{Q},\hat{E}},\tag{4.15}$$

using that $\nabla\phi_1=(DF_E^{-1})^T\hat{\nabla}\hat{\phi}_1$ in the second equality. Note that $\hat{\phi}_1$ is a trilinear function. Let $\tilde{\phi}_1$ be the linear part of $\hat{\phi}_1$. We have

$$(\hat{\Pi}_*\hat{\mathbf{u}}-\hat{\mathbf{u}}_h,\hat{\nabla}\hat{\phi}_1)_{\hat{Q},\hat{E}}=(\hat{\Pi}_*\hat{\mathbf{u}}-\hat{\mathbf{u}}_h,\hat{\nabla}(\hat{\phi}_1-\tilde{\phi}_1))_{\hat{Q},\hat{E}}+(\hat{\Pi}_*\hat{\mathbf{u}}-\hat{\mathbf{u}}_h,\hat{\nabla}\tilde{\phi}_1)_{\hat{Q},\hat{E}}.\tag{4.16}$$

Using (2.8), a direct calculation shows that

$$\hat{\nabla}(\hat{\phi}_1-\tilde{\phi}_1)=(DF_E(\hat{\mathbf{x}})-[\mathbf{r}_{21},\mathbf{r}_{41},\mathbf{r}_{51}])^T\nabla\phi_1,$$

where DF_E is defined in (3.2). Using that E is an h^2-parallelepiped, we have

$$\begin{aligned}|(\hat{\Pi}_*\hat{\mathbf{u}}-\hat{\mathbf{u}}_h,\hat{\nabla}(\hat{\phi}_1-\tilde{\phi}_1))_{\hat{Q},\hat{E}}|&\le Ch^2\|\hat{\Pi}_*\hat{\mathbf{u}}-\hat{\mathbf{u}}_h\|_{\hat{E}}\|\nabla\phi_1\|_{\hat{E}}\\&\le Ch^2h^{1/2}\|\Pi_*\mathbf{u}-\mathbf{u}_h\|_E h^{-3/2}\|\nabla\phi_1\|_E\\&\le Ch\|\Pi_*\mathbf{u}-\mathbf{u}_h\|_E\|\phi\|_{2,E},\end{aligned}\tag{4.17}$$

where we have used (3.5) in the second inequality. For the last term in (4.16), using (2.39) and the fact that the trapezoidal rule is exact for linear functions, we obtain

$$\begin{aligned}(\hat{\Pi}_*\hat{\mathbf{u}}-\hat{\mathbf{u}}_h,\hat{\nabla}\tilde{\phi}_1)_{\hat{Q},\hat{E}}&=(\hat{\Pi}_0(\hat{\Pi}_*\hat{\mathbf{u}}-\hat{\mathbf{u}}_h),\hat{\nabla}\tilde{\phi}_1)_{\hat{Q},\hat{E}}=(\hat{\Pi}_0(\hat{\Pi}_*\hat{\mathbf{u}}-\hat{\mathbf{u}}_h),\hat{\nabla}\tilde{\phi}_1)_{\hat{E}}\\&=(\hat{\Pi}_0(\hat{\Pi}_*\hat{\mathbf{u}}-\hat{\mathbf{u}}_h),\hat{\nabla}(\tilde{\phi}_1-\hat{\phi}_1)_{\hat{E}}+(\hat{\Pi}_0(\hat{\Pi}_*\hat{\mathbf{u}}-\hat{\mathbf{u}}_h),\hat{\nabla}\hat{\phi}_1)_{\hat{E}}.\end{aligned}\tag{4.18}$$

We bound the first term on the right in (4.18) in a way similar to (4.17):

$$|(\hat{\Pi}_0(\hat{\Pi}_*\hat{\mathbf{u}}-\hat{\mathbf{u}}_h),\hat{\nabla}(\tilde{\phi}_1-\hat{\phi}_1)_{\hat{E}}|\le Ch\|\Pi_*\mathbf{u}-\mathbf{u}_h\|_E\|\phi\|_{2,E}.\tag{4.19}$$

For the second term on the right in (4.18) we have

$$(\hat{\Pi}_0(\hat{\Pi}_*\hat{\mathbf{u}}-\hat{\mathbf{u}}_h),\hat{\nabla}\hat{\phi}_1)_{\hat{E}}=(\Pi_0(\Pi_*\mathbf{u}-\mathbf{u}_h),\nabla\phi_1)_E.\tag{4.20}$$

Combining (4.10)–(4.20), summing over all elements, and using (3.38), we obtain

$$(K^{-1}(\Pi_*\mathbf{u}-\mathbf{u}_h),\Pi_0K\nabla\phi)_Q=R+\sum_{E\in\mathcal{T}_h}(\Pi_0(\Pi_*\mathbf{u}-\mathbf{u}_h),\nabla\phi_1)_E,\tag{4.21}$$

where

$$|R|\le Ch^2\|\mathbf{u}\|_1\|\phi\|_2.\tag{4.22}$$

For the last term in (4.21), using the regularity of ϕ, (3.37), (2.22), and that $(\Pi_*\mathbf{u}-\mathbf{u}_h)\cdot\mathbf{n}=0$ on Γ_N and $\phi=0$ on Γ_D, we obtain

$$\begin{aligned}\left|\sum_{E\in\mathcal{T}_h}(\Pi_0(\Pi_*\mathbf{u}-\mathbf{u}_h),\nabla\phi_1)_E\right|&=\left|\sum_{E\in\mathcal{T}_h}(\Pi_0(\Pi_*\mathbf{u}-\mathbf{u}_h),\nabla(\phi_1-\phi))_E\right|\\&\le C\sum_{E\in\mathcal{T}_h}\|\Pi_*\mathbf{u}-\mathbf{u}_h\|_E\|\phi_1-\phi\|_{1,E}\\&\le Ch^2|||K^{-1}|||_{1,\infty}\|\mathbf{u}\|_1\|\phi\|_2,\end{aligned}\tag{4.23}$$

where we have also used (3.38) and (4.11). The proof of (4.4) is completed by combining (4.7)–(4.9) and (4.21)–(4.23) and using (4.5). ∎

Remark 4.1. Since $|p(m_E) - \mathcal{Q}_h p| \leq Ch^2$, where m_E is the center of mass of an element E, the above theorem implies that

$$|\!|\!| p - p_h |\!|\!| \leq Ch^2,$$

where $|\!|\!|\varphi|\!|\!| = (\sum_E |E| \varphi(m_E)^2)^{1/2}$.

5. Numerical experiments. In this section we provide several numerical experiments that confirm the theoretical results from the previous sections. For all experiments, K is a full tensor with variable entries,

$$K = \begin{pmatrix} x^2 + (y+2)^2 & 0 & \cos(xy) \\ 0 & z^2 + 2 & \sin(yz) \\ \cos(xy) & \sin(yz) & (y+3)^2 \end{pmatrix}.$$

We solve a problem of type (2.1)–(2.3) with Dirichlet boundary conditions and a known solution

$$p = x^4 y^3 + x^2 + yz^2 + \cos(xy) + \sin(z).$$

We present three examples with varying smoothness of the grids. In each example we test the convergence of our method on $2^k \times 2^k \times 2^k$ grids for $k = 3, 4, 5, 6$. To handle the large amount of memory required in these computations, the problem domains are split into eight equally partitioned subdomains of size $2^k \times 2^k \times 2^k$ for $k = 2, 3, 4, 5$, and the problem is solved in parallel. The discretization errors and convergence rates at each level of refinement are provided for each example. The error norms $\|p - p_h\|$, $\|\mathbf{u} - \mathbf{u}_h\|$, and $\|\nabla \cdot (\mathbf{u} - \mathbf{u}_h)\|$ are computed by an element-by-element trapezoid quadrature rule. In addition, we report convergence for $|\!|\!| p - p_h |\!|\!|$ and $|\!|\!| \mathbf{u} - \mathbf{u}_h |\!|\!|$, which represent an approximation of the L^2-norm obtained by an element-by-element midpoint quadrature rule. In the tables below R_p^h, $R_{\mathbf{u}}^h$, $R_{\nabla\cdot\mathbf{u}}^h$, $\tilde{R}_p^h$, and $\tilde{R}_{\mathbf{u}}^h$ represent the convergence rate between two refinements for the errors $\|p - p_h\|$, $\|\mathbf{u} - \mathbf{u}_h\|$, $\|\nabla \cdot (\mathbf{u} - \mathbf{u}_h)\|$, $|\!|\!| p - p_h |\!|\!|$, and $|\!|\!| \mathbf{u} - \mathbf{u}_h |\!|\!|$, respectively; e.g.,

$$R_p^h = \frac{\log\left(\left\|p - p_{h/2}\right\| / \|p - p_h\|\right)}{\log(2)}.$$

In example 1, we take the domain to be a C^∞ map of the unit cube. The map is defined as

$$\begin{aligned} x &= \hat{x} + 0.03 \cos(3\pi\hat{x}) \cos(3\pi\hat{y}) \cos(3\pi\hat{z}), \\ y &= \hat{y} - 0.04 \cos(3\pi\hat{x}) \cos(3\pi\hat{y}) \cos(3\pi\hat{z}), \\ z &= \hat{z} + 0.05 \cos(3\pi\hat{x}) \cos(3\pi\hat{y}) \cos(3\pi\hat{z}). \end{aligned}$$

The computational grids on the different levels are defined by mapping uniform refinements of a reference grid on the unit cube. More precisely, each element is defined via a trilinear map that approximates locally the smooth map defined above. Due to the smoothness of the global map, the elements are regular h^2-parallelepipeds. The computed solution and its error on the second grid level are shown in Figure 4. The convergence data is presented in Table 1. As predicted by the theory, we observe

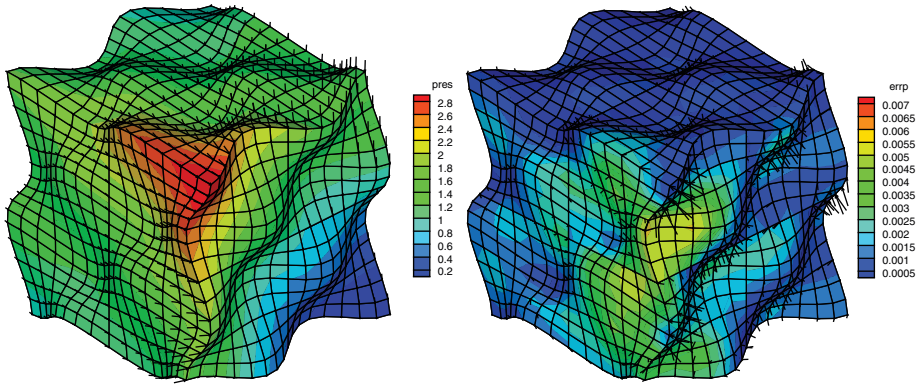

FIG. 4. $16 \times 16 \times 16$ *discretization on a smooth grid in example* 1: *MFMFE solution (left), MFMFE error (right).*

TABLE 1
Discretization errors and convergence rates for example 1.

MFMFE-Method										
$1/h$	$\|p-p_h\|$	R_p^h	$\|\mathbf{u}-\mathbf{u}_h\|$	$R_{\mathbf{u}}^h$	$\|\nabla\cdot(\mathbf{u}-\mathbf{u}_h)\|$	$R_{\nabla\cdot\mathbf{u}}^h$	$\|\!\|p-p_h\|\!\|$	$\tilde{R}_p^h$	$\|\!\|\mathbf{u}-\mathbf{u}_h\|\!\|$	$\tilde{R}_{\mathbf{u}}^h$
8	0.120E0		0.164E0		0.188E0		0.549E-2		0.508E-1	
16	0.605E-1	1.0	0.834E-1	1.0	0.941E-1	1.0	0.182E-2	1.6	0.212E-1	1.3
32	0.304E-1	1.0	0.417E-1	1.0	0.470E-1	1.0	0.496E-3	1.9	0.610E-1	1.8
64	0.152E-1	1.0	0.208E-1	1.0	0.235E-1	1.0	0.127E-3	2.0	0.159E-1	1.9
EMFE-Method										
$1/h$	$\|p-p_h\|$	R_p^h	$\|\mathbf{u}-\mathbf{u}_h\|$	$R_{\mathbf{u}}^h$	$\|\nabla\cdot(\mathbf{u}-\mathbf{u}_h)\|$	$R_{\nabla\cdot\mathbf{u}}^h$	$\|\!\|p-p_h\|\!\|$	$\tilde{R}_p^h$	$\|\!\|\mathbf{u}-\mathbf{u}_h\|\!\|$	$\tilde{R}_{\mathbf{u}}^h$
8	0.120E0		0.177E0		0.188E0		0.594E-2		0.542E-1	
16	0.606E-1	1.0	0.970E-1	0.8	0.941E-1	1.0	0.232E-2	1.4	0.231E-1	1.2
32	0.304E-1	1.0	0.500E-1	0.9	0.470E-1	1.0	0.696E-3	1.7	0.695E-1	1.7
64	0.152E-1	1.0	0.252E-1	1.0	0.235E-1	1.0	0.188E-3	1.9	0.192E-1	1.8

first-order convergence for the pressure, the velocity, and its divergence as well as second-order convergence for the pressure at the cell centers. Moreover, the velocity also converges with second-order at the cell centers. In Table 1 we also report the convergence for the EMFE method. Since the grids are globally smooth, the MFMFE method and the EMFE method perform in a comparable way.

In example 2, we take the domain to be a random perturbation of an initial uniform $4 \times 4 \times 4$ partition of the unit cube. More precisely, each grid point is moved randomly between $-1/3$ and $1/3$ in each direction. The computational grids are uniform refinements of this initial rough grid. The resulting elements are regular h^2-parallelepipeds. Note that the nonsmoothness of the grid translates into a discontinuous reference permeability $\mathcal{K}$; see (2.31). The computed solution and its error on the second grid level are shown in Figure 5. The convergence data in Table 2 confirms the theoretical results. In particular, we observe first-order convergence for the pressure, the velocity, and its divergence as well as second-order convergence for the pressure at the cell centers. As in the smooth grids example, the velocity also exhibits superconvergence at the cell centers, although in this case the rate is slightly reduced to $O(h^{1.5})$. We again compare the MFMFE method to the EMFE method. The computed EMFE solution and its error on the second grid level are shown in Figure 6. The data for the EMFE method in Table 2 indicates reduced order conver-

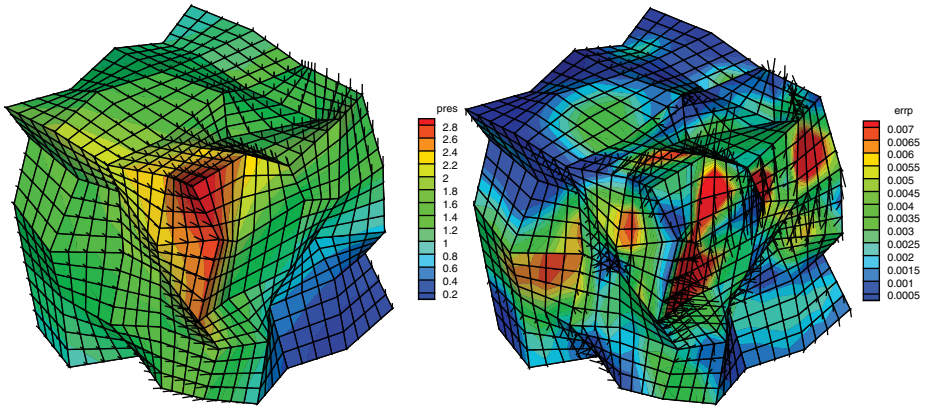

FIG. 5. $16 \times 16 \times 16$ *discretization on a rough grid in example* 2: *MFMFE solution (left), MFMFE error (right).*

TABLE 2
Discretization errors and convergence rates for example 2.

MFMFE-Method										
$1/h$	$\|p-p_h\|$	R_p^h	$\|\mathbf{u}-\mathbf{u}_h\|$	$R_{\mathbf{u}}^h$	$\|\nabla\cdot(\mathbf{u}-\mathbf{u}_h)\|$	$R_{\nabla\cdot\mathbf{u}}^h$	$\|\|\|p-p_h\|\|\|$	$\tilde{R}_p^h$	$\|\|\|\mathbf{u}-\mathbf{u}_h\|\|\|$	$\tilde{R}_{\mathbf{u}}^h$
8	0.129E0		0.280E0		0.187E0		0.105E-1		0.895E-1	
16	0.638E-1	1.0	0.125E0	1.1	0.937E-1	1.0	0.366E-2	1.5	0.374E-1	1.3
32	0.318E-1	1.0	0.590E-1	1.1	0.468E-1	1.0	0.107E-2	1.8	0.122E-1	1.6
64	0.159E-1	1.0	0.296E-1	1.0	0.234E-1	1.0	0.283E-3	1.9	0.410E-2	1.6
EMFE-Method										
$1/h$	$\|p-p_h\|$	R_p^h	$\|\mathbf{u}-\mathbf{u}_h\|$	$R_{\mathbf{u}}^h$	$\|\nabla\cdot(\mathbf{u}-\mathbf{u}_h)\|$	$R_{\nabla\cdot\mathbf{u}}^h$	$\|\|\|p-p_h\|\|\|$	$\tilde{R}_p^h$	$\|\|\|\mathbf{u}-\mathbf{u}_h\|\|\|$	$\tilde{R}_{\mathbf{u}}^h$
8	0.128E0		0.225E0		0.187E0		0.992E-2		0.965E-1	
16	0.638E-1	1.0	0.129E0	0.8	0.937E-1	1.0	0.434E-2	1.1	0.536E-1	0.8
32	0.318E-1	1.0	0.708E-1	0.8	0.468E-1	1.0	0.170E-2	1.4	0.338E-1	0.7
64	0.159E-1	1.0	0.410E-1	0.8	0.234E-1	1.0	0.651E-3	1.4	0.258E-1	0.4

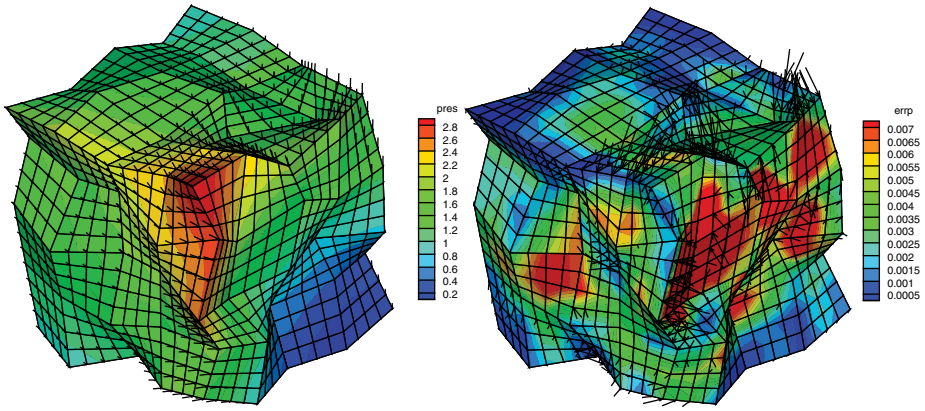

FIG. 6. $16 \times 16 \times 16$ *discretization on a rough grid in example* 2: *EMFE solution (left), EMFE error (right).*

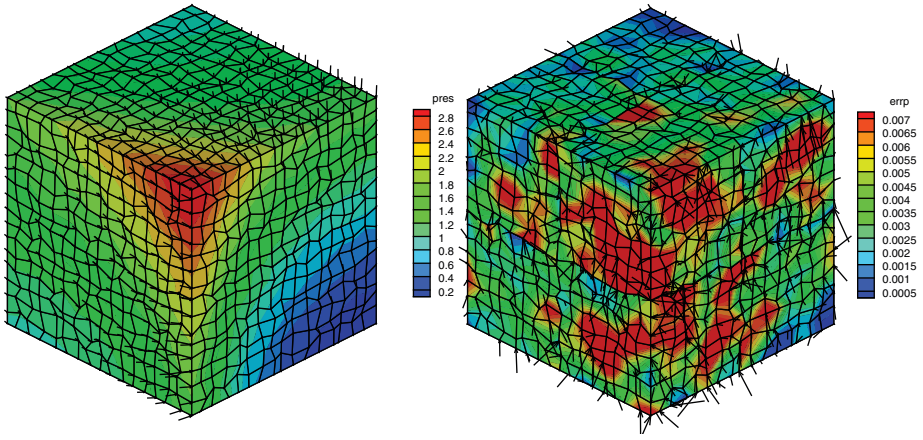

FIG. 7. $16\times16\times16$ *discretization on a random* $O(h)$ *refinement in example* 3: *MFMFE solution (left), MFMFE error (right).*

TABLE 3
Discretization errors and convergence rates for the MFMFE method in example 3.

$O\left(h^2\right)$-Refinements										
$1/h$	$\|p-p_h\|$	R_p^h	$\|\mathbf{u}-\mathbf{u}_h\|$	$R_{\mathbf{u}}^h$	$\|\nabla\cdot(\mathbf{u}-\mathbf{u}_h)\|$	$R_{\nabla\cdot\mathbf{u}}^h$	$\|\!\|p-p_h\|\!\|$	$\tilde{R}_p^h$	$\|\!\|\mathbf{u}-\mathbf{u}_h\|\!\|$	$\tilde{R}_{\mathbf{u}}^h$
8	0.118E0		0.104E0		0.190E0		0.549E-2		0.508E-1	
16	0.584E-1	1.0	0.529E-1	1.0	0.958E-1	1.0	0.182E-2	2.0	0.212E-1	1.0
32	0.291E-1	1.0	0.265E-1	1.0	0.480E-1	1.0	0.496E-3	2.0	0.610E-1	1.0
64	0.146E-1	1.0	0.133E-1	1.0	0.240E-1	1.0	0.127E-3	2.0	0.159E-1	1.0
$O\left(h^{1.5}\right)$-Refinements										
$1/h$	$\|p-p_h\|$	R_p^h	$\|\mathbf{u}-\mathbf{u}_h\|$	$R_{\mathbf{u}}^h$	$\|\nabla\cdot(\mathbf{u}-\mathbf{u}_h)\|$	$R_{\nabla\cdot\mathbf{u}}^h$	$\|\!\|p-p_h\|\!\|$	$\tilde{R}_p^h$	$\|\!\|\mathbf{u}-\mathbf{u}_h\|\!\|$	$\tilde{R}_{\mathbf{u}}^h$
8	0.119E0		0.170E0		0.191E0		0.538E-2		0.346E-1	
16	0.587E-1	1.0	0.118E-1	0.5	0.961E-1	1.0	0.158E-2	1.8	0.266E-1	0.4
32	0.292E-1	1.0	0.816E-1	0.5	0.481E-1	1.0	0.507E-3	1.6	0.191E-1	0.5
64	0.146E-1	1.0	0.569E-1	0.5	0.240E-1	1.0	0.173E-3	1.5	0.138E-1	0.5
$O\left(h\right)$-Refinements										
$1/h$	$\|p-p_h\|$	R_p^h	$\|\mathbf{u}-\mathbf{u}_h\|$	$R_{\mathbf{u}}^h$	$\|\nabla\cdot(\mathbf{u}-\mathbf{u}_h)\|$	$R_{\nabla\cdot\mathbf{u}}^h$	$\|\!\|p-p_h\|\!\|$	$\tilde{R}_p^h$	$\|\!\|\mathbf{u}-\mathbf{u}_h\|\!\|$	$\tilde{R}_{\mathbf{u}}^h$
8	0.120E0		0.726E0		0.196E0		0.110E-1		0.100E-1	
16	0.630E-1	1.0	0.155E+1	—	0.100E0	1.0	0.597E-2	0.9	0.112E-1	—
32	0.316E-1	1.0	0.692E-1	—	0.501E-1	1.0	0.391E-2	0.6	0.115E-1	—
64	0.161E-1	1.0	0.775E0	—	0.251E-1	1.0	0.327E-2	0.3	0.119E-1	—

gence for the velocity as well as for the pressure and velocity at the cell centers. This is expected, as it is known that the EMFE method suffers from reduction in accuracy on rough grids or discontinuous coefficients [4]. It can be seen in Figure 6 that the velocity error for the EMFE method is quite large where the grid is rough.

In example 3, the domain is the unit cube and the grids are defined by random $O\left(h^s\right)$-perturbations of uniform refinements for $s = 2$, 1.5, and 1. The goal here is to study the dependence of the MFMFE convergence rates on the regularity of the grids. The computed solution and its error on the second grid level for case $s = 1$ are shown in Figure 7. The convergence data is given in Table 3. In the case of $O\left(h^2\right)$-perturbed refinements, the elements are regular h^2-parallelepipeds, and we observe $O\left(h\right)$-convergence for $\|p-p_h\|$, $\|\mathbf{u}-\mathbf{u}_h\|$, and $\|\nabla\cdot(\mathbf{u}-\mathbf{u}_h)\|$ as well as $O\left(h^2\right)$-convergence for the pressure and the velocity at the cell centers. The pressure

also converges with first-order for $O(h^s)$-perturbed refinements when $s < 2$, but the optimal velocity convergence is lost as well as the superconvergence of the pressure and velocity in the discrete cell-centered L^2-norms. Note that the convergence deteriorates when the scale of the random perturbations is increased; no velocity convergence is observed for $O(h)$-perturbed refinements.

In summary, the numerical experiments confirm the theoretical convergence results for the MFMFE method. In addition, the MFMFE method performs favorably on rough grids compared to the EMFE method, which suffers a reduction in the convergence rate.

Acknowledgments. The authors thank Guangri Xue for suggesting to use in the scheme the piecewise constant projection of the boundary Dirichlet data and other valuable discussions.

REFERENCES

[1] I. Aavatsmark, *An introduction to multipoint flux approximations for quadrilateral grids*, Comput. Geosci., 6 (2002), pp. 405–432.

[2] I. Aavatsmark, T. Barkve, Ø. Bøe, and T. Mannseth, *Discretization on unstructured grids for inhomogeneous, anisotropic media. Part* I. *Derivation of the methods*, SIAM J. Sci. Comput., 19 (1998), pp. 1700–1716.

[3] I. Aavatsmark, G. T. Eigestad, R. A. Klausen, M. F. Wheeler, and I. Yotov, *Convergence of a symmetric MPFA method on quadrilateral grids*, Comput. Geosci., 11 (2007), pp. 333–345.

[4] T. Arbogast, C. N. Dawson, P. T. Keenan, M. F. Wheeler, and I. Yotov, *Enhanced cell-centered finite differences for elliptic equations on general geometry*, SIAM J. Sci. Comput., 19 (1998), pp. 404–425.

[5] T. Arbogast, M. F. Wheeler, and I. Yotov, *Mixed finite elements for elliptic problems with tensor coefficients as cell-centered finite differences*, SIAM J. Numer. Anal., 34 (1997), pp. 828–852.

[6] D. N. Arnold, D. Boffi, and R. S. Falk, *Quadrilateral H(div) finite elements*, SIAM J. Numer. Anal., 42 (2005), pp. 2429–2451.

[7] D. N. Arnold and F. Brezzi, *Mixed and nonconforming finite element methods: Implementation, postprocessing and error estimates*, RAIRO Model. Math. Anal. Numer., 19 (1985), pp. 7–32.

[8] J. Baranger, J.-F. Maitre, and F. Oudin, *Connection between finite volume and mixed finite element methods*, RAIRO Model. Math. Anal. Numer., 30 (1996), pp. 445–465.

[9] M. Berndt, K. Lipnikov, J. D. Moulton, and M. Shashkov, *Convergence of mimetic finite difference discretizations of the diffusion equation*, J. Numer. Math., 9 (2001), pp. 253–284.

[10] M. Berndt, K. Lipnikov, M. Shashkov, M. F. Wheeler, and I. Yotov, *A mortar mimetic finite difference method on non-matching grids*, Numer. Math., 102 (2005), pp. 203–230.

[11] M. Berndt, K. Lipnikov, M. Shashkov, M. F. Wheeler, and I. Yotov, *Superconvergence of the velocity in mimetic finite difference methods on quadrilaterals*, SIAM J. Numer. Anal., 43 (2005), pp. 1728–1749.

[12] S. C. Brenner and L. R. Scott, *The Mathematical Theory of Finite Element Methods*, Texts Appl. Math. 15, Springer-Verlag, New York, 2002.

[13] F. Brezzi, J. Douglas, Jr., R. Durán, and M. Fortin, *Mixed finite elements for second order elliptic problems in three variables*, Numer. Math., 51 (1987), pp. 237–250.

[14] F. Brezzi, J. Douglas, Jr., and L. D. Marini, *Two families of mixed elements for second order elliptic problems*, Numer. Math., 88 (1985), pp. 217–235.

[15] F. Brezzi and M. Fortin, *Mixed and Hybrid Finite Element Methods*, Springer Ser. Comput. Math. 15, Springer-Verlag, Berlin, 1991.

[16] F. Brezzi, M. Fortin, and L. D. Marini, *Error analysis of piecewise constant pressure approximations of Darcy's law*, Comput. Methods Appl. Mech. Engrg., 195 (2006), pp. 1547–1559.

[17] F. Brezzi, K. Lipnikov, and M. Shashkov, *Convergence of mimetic finite difference method for diffusion problems on polyhedral meshes*, SIAM J. Numer. Anal., 43 (2005), pp. 1872–1896.

[18] Z. Cai, J. E. Jones, S. F. McCormick, and T. F. Russell, *Control-volume mixed finite element methods*, Comput. Geosci., 1 (1997), pp. 289–315.
[19] S.-H. Chou, D. Y. Kwak, and K. Y. Kim, *A general framework for constructing and analyzing mixed finite volume methods on quadrilateral grids: The overlapping covolume case*, SIAM J. Numer. Anal., 39 (2001), pp. 1170–1196.
[20] P. G. Ciarlet, *The Finite Element Method for Elliptic Problems*, North-Holland, New York, 1978.
[21] M. G. Edwards, *Unstructured, control-volume distributed, full-tensor finite-volume schemes with flow based grids*, Comput. Geosci., 6 (2002), pp. 433–452.
[22] M. G. Edwards and C. F. Rogers, *Finite volume discretization with imposed flux continuity for the general tensor pressure equation*, Comput. Geosci., 2 (1998), pp. 259–290.
[23] R. Eymard, T. Gallouët, and R. Herbin, *Finite volume methods*, Handb. Numer. Anal. 7, North-Holland, Amsterdam, 2000, pp. 713–1020.
[24] R. Eymard, T. Gallouët, and R. Herbin, *A new finite volume scheme for anisotropic diffusion problems on general grids: Convergence analysis*, C. R. Math. Acad. Sci. Paris, 344 (2007), pp. 403–406.
[25] G. P. Galdi, *An introduction to the mathematical theory of the Navier-Stokes equations. Vol.* I: *Linearized Steady Problems*, Springer-Verlag, New York, 1994.
[26] V. Girault and P.-A. Raviart, *Finite element methods for Navier-Stokes equations, Theory and algorithms*, Springer-Verlag, Berlin, 1986.
[27] P. Grisvard, *Elliptic Problems in Nonsmooth Domains*, Pitman, Boston, 1985.
[28] J. M. Hyman, M. Shashkov, and S. Steinberg, *The numerical solution of diffusion problems in strongly heterogeneous non-isotropic materials*, J. Comput. Phys., 132 (1997), pp. 130–148.
[29] R. A. Klausen and T. F. Russell, *Relationships among some locally conservative discretization methods which handle discontinuous coefficients*, Comput. Geosci., 8 (2004), pp. 341–377.
[30] R. A. Klausen and R. Winther, *Convergence of multipoint flux approximations on quadrilateral grids*, Numer. Methods Partial Differential Equations, 22 (2006), pp. 1438–1454.
[31] R. A. Klausen and R. Winther, *Robust convergence of multi point flux approximation on rough grids*, Numer. Math., 104 (2006), pp. 317–337.
[32] Y. Kuznetsov and S. Repin, *New mixed finite element method on polygonal and polyhedral meshes*, Russ. J. Numer. Anal. Math. Modelling, 18 (2003), pp. 261–278.
[33] Y. Kuznetsov and S. Repin, *Convergence analysis and error estimates for mixed finite element method on distorted meshes*, J. Numer. Math., 13 (2005), pp. 33–51.
[34] J. L. Lions and E. Magenes, *Non-Homogeneous Boundary Value Problems and Applications*, Vol. 1, Springer-Verlag, Berlin, 1972.
[35] K. Lipnikov, M. Shashkov, and I. Yotov, *Local flux mimetic finite difference methods*, Numer. Math., 112 (2009), pp. 115–152.
[36] R. L. Naff, T. F. Russell, and J. D. Wilson, *Shape functions for velocity interpolation in general hexahedral cells*, Comput. Geosci., 6 (2002), pp. 285–314.
[37] J. C. Nedelec, *Mixed finite elements in* $\mathbf{R}^3$, Numer. Math., 35 (1980), pp. 315–341.
[38] R. A. Raviart and J. M. Thomas, *A mixed finite element method for* 2*nd order elliptic problems*, in Mathematical Aspects of the Finite Element Method, Lecture Notes in Math. 606, Springer-Verlag, New York, 1977, pp. 292–315.
[39] J. E. Roberts and J. M. Thomas, *Mixed and Hybrid Methods*, Handb. Numer. Anal. 2, P. Ciarlet and J. Lions, eds., Elsevier/North Holland, Amsterdam, 1991.
[40] T. F. Russell and M. F. Wheeler, *Finite element and finite difference methods for continuous flows in porous media*, in The Mathematics of Reservoir Simulation, R. E. Ewing, ed., Frontiers Appl. Math. 1, SIAM, Philadelphia, 1983, pp. 35–106.
[41] T. F. Russell, M. F. Wheeler, and I. Yotov, *Superconvergence for control-volume mixed finite element methods on rectangular grids*, SIAM J. Numer. Anal., 45 (2007), pp. 223–235.
[42] A. Sboui, J. Jaffré, and J. E. Roberts, *A composite mixed finite element for general hexahedral grids*, SIAM J. Sci. Comput., to appear.
[43] A. H. Stroud, *Approximate Calculation of Multiple Integrals*, Prentice-Hall, Englewood Cliffs, NJ, 1971.
[44] J. M. Thomas, *These de Doctorat d'etat*, 'a l'Universite Pierre et Marie Curie, Paris, 1977.
[45] J. Wang and T. P. Mathew, *Mixed finite element method over quadrilaterals*, in Conference on Advances in Numerical Methods and Applications, I. T. Dimov, B. Sendov, and P. Vassilevski, eds., World Scientific, River Edge, NJ, 1994, pp. 203–214.
[46] A. Weiser and M. F. Wheeler, *On convergence of block-centered finite differences for elliptic problems*, SIAM J. Numer. Anal., 25 (1988), pp. 351–375.

[47] M. F. Wheeler and I. Yotov, *A cell-centered finite difference method on quadrilaterals*, in Compatible Spatial Discretizations, IMA Vol. Math. Appl. 142, Springer-Verlag, New York, 2006, pp. 189–207.
[48] M. F. Wheeler and I. Yotov, *A multipoint flux mixed finite element method*, SIAM J. Numer. Anal., 44 (2006), pp. 2082–2106.
[49] A. Younes, P. Ackerer, and G. Chavent, *From mixed finite elements to finite volumes for elliptic PDEs in two and three dimensions*, Internat. J. Numer. Methods Engrg., 59 (2004), pp. 365–388.